自己集合性中空錯体の孤立ナノ空間内における ペプチドの認識

(Peptide Recognition within the Nano-sized Cavities of Self-assembled Coordination Receptors)

Department of Applied Chemistry
School of Engineering
The University of Tokyo

Shohei TASHIRO

2006

Contents

Chapter 1

General Introduction

1.1 Molecular Recognition

Molecular recognition is considered as one of the most fundamental phenomena in chemistry and biology.[1] Receptor (host) molecules bind guest molecules in solution. The driving force of guest binding is various interactions such as hydrogen bonding, electrostatic interaction and hydrophobic effect between receptors and guest molecules. Thus, various receptors for the recognition of cations, anions, and neutral organic molecules have been synthesized based on the rational design of such interactions.

Crown ethers, reported by Pedersen in 1967, are cyclic polyether derivatives that can bind cations, especially alkaline earth metals, Li^+, Na^+ and K^+ through ion-dipole interaction.[2] Three-dimensional crown-ethers (cryptands) accommodate cations more strongly than crown ethers.[3] On the other hand, cyclic polyamines are effective anion receptors. Protonated cyclic polyamines bind some halogen ions through hydrogen bonding.[4] Neutral organic molecules are also recognized by cyclodextrins,[5] calixarenes,[6] and carcerands[7] (Figure 1). Recently, some molecular capsules possessing a relatively large binding pocket are constructed by self-assembly via hydrogen bonding and coordination.[8,9]

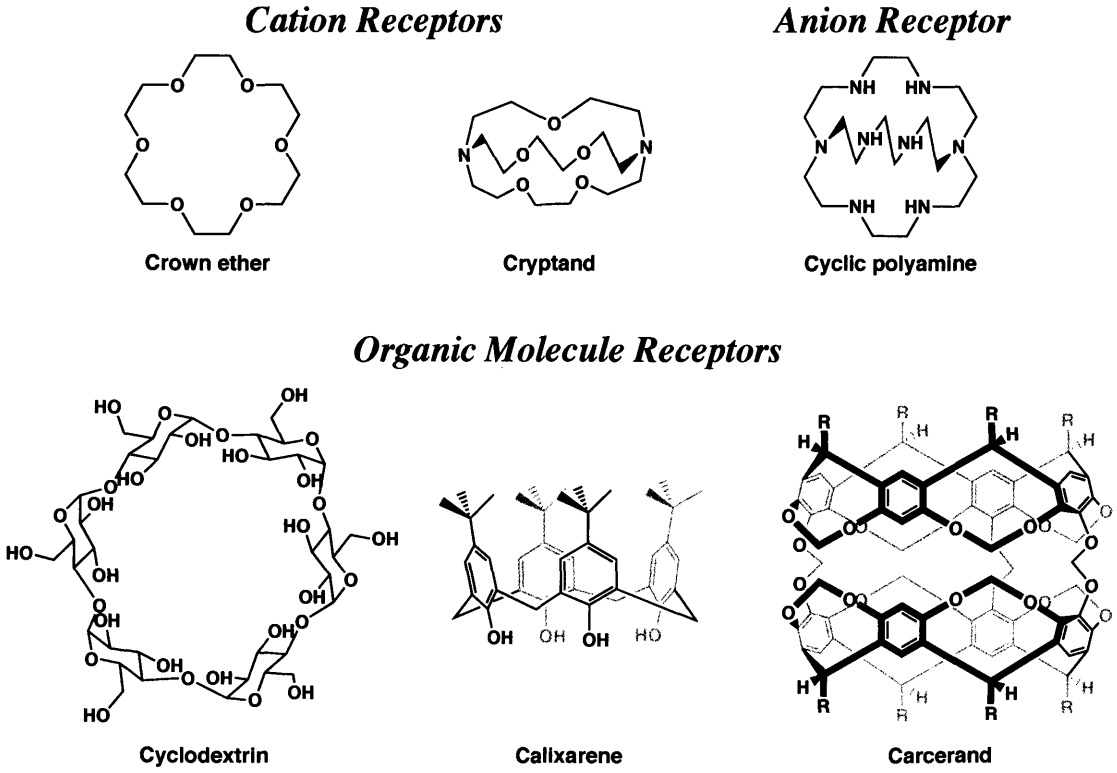

Figure 1. Chemical structures of cation, anion and organic molecule receptors.

1.2 Peptide Recognition

1.2.1 Importance of the peptide recognition (1): regulation of protein-protein interaction

Today, peptides are considered as extremely important targets in molecular recognition.[10] If peptide receptors can recognize specific peptide sequences, these receptors are expected to regulate various vital functions.[11] Regulation of protein-protein interaction is one of the most useful applications of peptide recognition.[12] Protein-protein interactions are known to play a critical role in the normal function of cellular/organelle structures, immune response, protein enzyme inhibitors, signal transduction and apoptosis.[13] Thus, when peptide receptors bind protein surface meditating the protein-protein interactions, the association of these proteins are inhibited and related vital functions are expected to be regulated (Figure 2).[14]

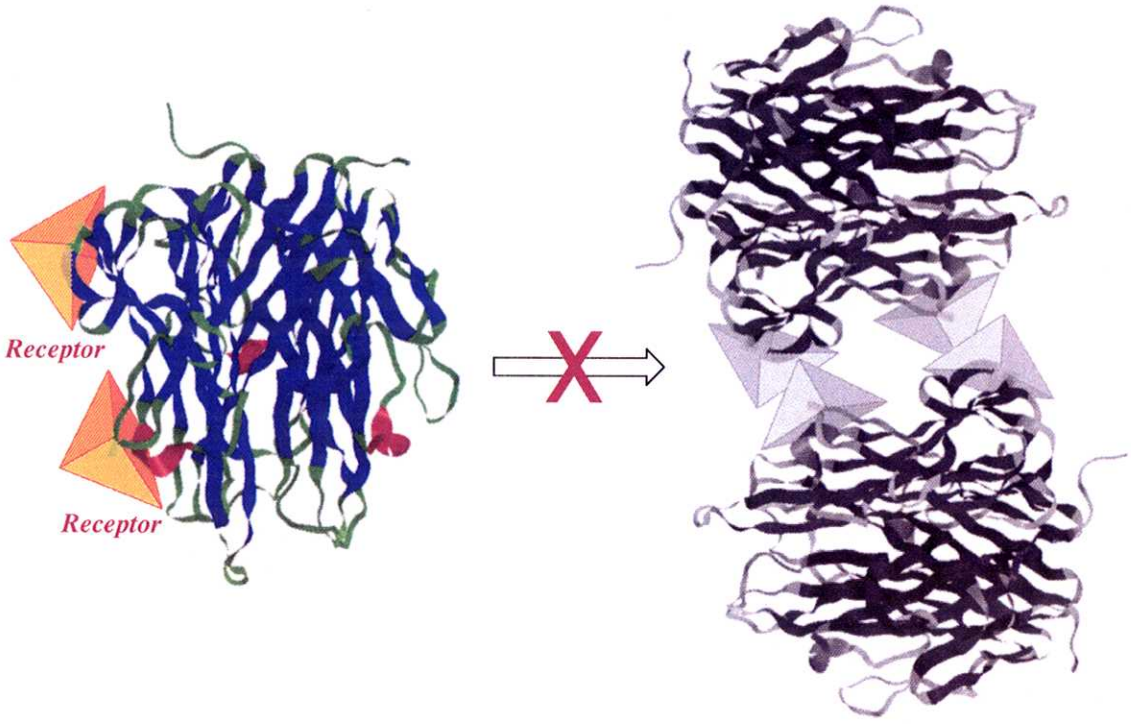

Figure 2. Schematic representation of the inhibition of the protein-protein interaction by the recognition of a protein surface by synthetic receptors.

For the effective binding of a protein surface, the selective recognition of peptide sequence is the most important approach.[15] A protein surface contains the unique distribution of amino acid residues possessing various functional groups (hydrophobic, hydrophilic, cationic, and anionic). In many cases, these regions are involved in important interactions with other proteins. Therefore, it is interesting to develop an artificial receptor that selectively

recognizes a specific peptide sequence on the protein surface mediating protein-protein interaction.

Some specific peptide sequences are known to regulate some protein interactions. For example, an Arg-Gly-Asp sequence on the solvent exposed loop of some growth factor proteins is related to cell-cell adhesion through interaction with a integrins, that is glycoprotein anchored inside a cell membrane.[16] On the other hand, a nucleation site for the pathogenic aggregation of the Alzheimer's peptide is identified as the Lys-Leu-Val-Phe-Phe sequence in the central region of Aβ.[17] Furthermore, a glycopeptide antibiotics, vancomycin binds to the C-terminal D-Ala-D-Ala sequences of peptidoglycan interamediates produced during bacterial cell wall biosynthesis (Figure 3).[18]

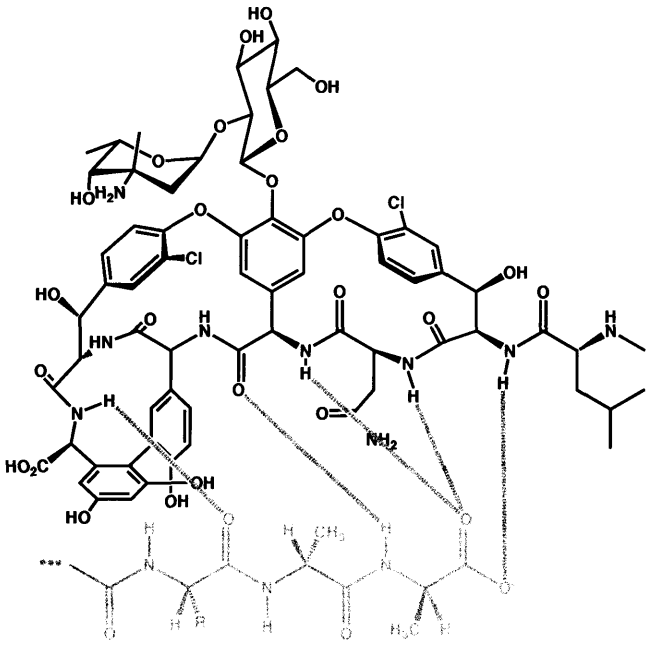

Figure 3. Chemical structures of vancomycin binding D-Ala-D-Ala sequences. Hydrogen bonds are emphasized.

1.2.2 Importance of the peptide recognition (2): control of protein tertiary structure

Another important aspect of peptides is the formation of a variety of secondary structures, like α-helix, β-sheet, and β-turn (Figure 4). Since proteins are composed of some peptide secondary structures, the control of peptide conformations seem to be directly concerned with stabilization or destabilization of protein tertiary structures. Furthermore, the formation of secondary structures is considered as a key step of protein folding.[19] Therefore, not only the selective recognition of peptide sequences, but also the stabilization of secondary structures

are important in peptide recognition.

As described above, there are mainly two current topics in peptide recognition, ***(1) selective recognition of peptide sequence***, and ***(2) control of peptide secondary structure via recognition***.

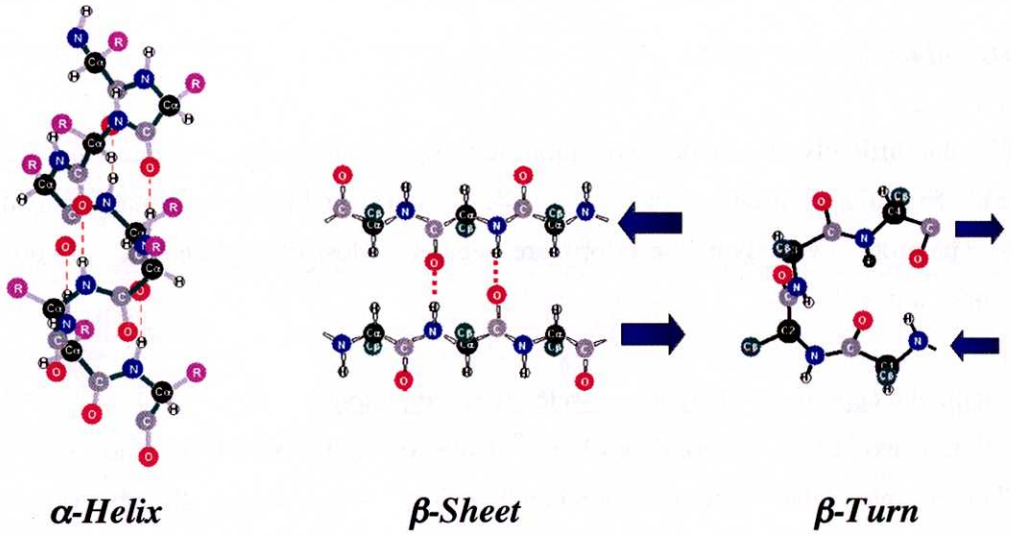

Figure 4. Chemical structure of peptide secondary structures, α-helix, β-sheet and β-turn.

1.2.3 Difficulty of the peptide recognition by artificial receptors

Although peptide recognition is expected to control various biological functions, peptides had been not treated as guest molecules in host-guest chemistry. The reason is the difficulty of peptide recognition. For the effective peptide recognition, we have to design and synthesize elaborate receptors as described below. At first, peptide is too large to be recognized by general artificial receptors. An oligopeptide chain possesses the size of nano-meter order. Secondly, peptides have various functional groups including hydrophobic, anionic, and cationic ones on their backbones. For the simultaneous recognition of their functional groups, peptide receptors must possess many recognition sites. Thirdly, the inherent flexibility and the structural diversity of peptides are fatal problems in peptide recognition. Since an amino acid residue has some free rotation bonds in a peptide backbone, polypeptide chain is inherently flexible. Peptides can also take various secondary structures such as α-helix, 3_{10}-helix, β-strand, β-hairpin, β-turn and γ-turn along with the peptide backbone. Therefore, for the rational peptide recognition, receptors must recognize not only their sequence, but also their conformations. Finally, peptide recognitions must be carried out in aqueous solution for biological applications. Peptides have a lot of hydrogen bonding

sites on its backbone and several charged side chains. Therefore, in some cases, peptide receptors use hydrogen bonding or electrostatic interaction as driving force of peptide recognition. However, their interactions become considerably weak in water. Additionally, some organic receptors show quite low solubility in water.

1.3 Design of Peptide Receptors

Despite the difficulty of peptide recognition, recently, several peptide receptors have been designed. Essentially, those receptors are made by covalent linking of some recognition sites.[20] Therefore severe synthetic efforts are needed. Most of peptide receptors do not work in pure water.

1.3.1 Peptide receptors for the sequence-selective recognition

Still and co-workers synthesized bowl-shaped macrotricyclic peptide receptor **1** (Figure 5).[21] This receptor **1** has some hydrogen-bonding sites. Thus, several di- and tri-peptides are bound in this receptor through hydrogen bonding. Receptor **1** recognizes some peptides with sequence-selectivity. However, this recognition occurs only in organic solvent such as chloroform.

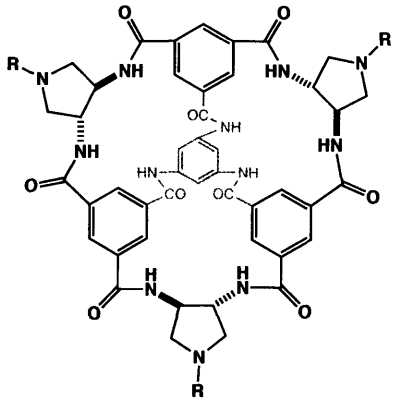

1

Figure 5. Chemical structure of bowl-shaped macrotricyclic peptide receptor **1** designed by Still and co-workers.

To recognize peptides in aqueous solution, multiple interaction between a receptor and a peptide is needed.[22] Schneider and co-workers designed elaborate peptide receptors possessing the multiple recognition sites. Receptor **2** has crown ether and ammonium ion at

the both terminals and aromatic moiety in the middle of **2** (Figure 6).[23] This receptor recognizes a tripeptide even in water due to their multiple interactions. The crown ether site of **2** binds the free N-terminal of peptide, and ammonium ion site of **2** recognizes the free C-terminal of the peptide. Furthermore, aromatic moiety of **2** stacks with aromatic side-chain of middle residue of peptide. Therefore, receptor **2** recognizes a free tripeptide, H-Gly-Trp-Gly-OH possessing aromatic residue Trp in the middle, with moderate affinity even in water ($K_a = 10^3\ M^{-1}$).

On the other hand, Schneider and co-workers synthesized receptor **3** containing porphyrin and crown ether moieties (Figure 6).[24] This receptor also recognizes a tripeptide H-Gly-Gly-Phe-OH by electrostatic interaction between N-terminal of the peptide and the crown ether of **3**, and by aromatic stacking between the phenyl ring of Phe3 and the porphyrin moiety of **3**. This recognition occurs even in water.

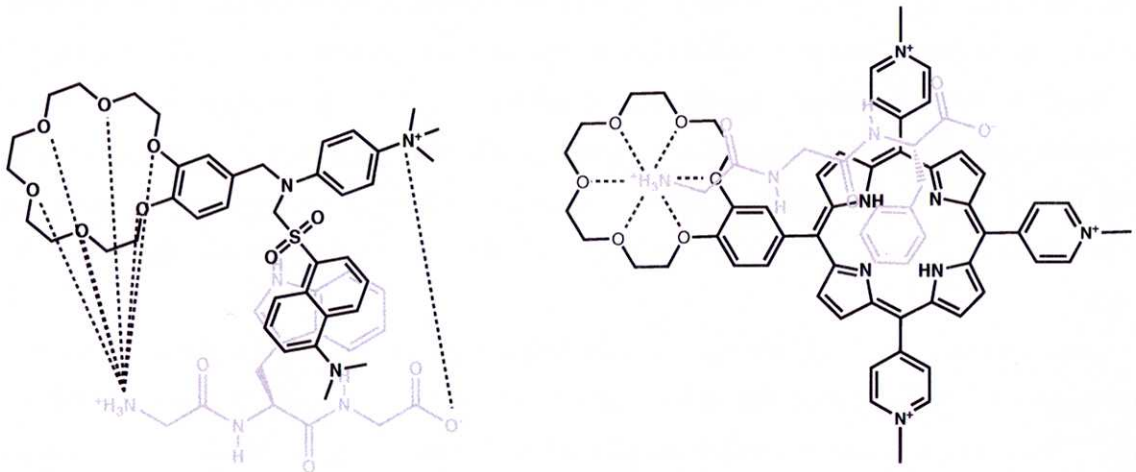

Figure 6. Chemical structures of receptor **2** and Gly-Trp-Gly (left) and receptor **3** and Gly-Gly-Phe (right) designed by Schneider and co-workers.

Schrader and co-workers designed receptor **4** for an Arg-Gly-Asp sequence, that is related to the cell-cell adhesion, by using the multiple interaction (Figure 7).[25] The three phosphonate arms of the **4** recognize the guanidium moiety of Arg residue, and ammonium moiety on the phenyl ring of **4** binds the carboxylate side-chain of Asp residue. This receptor **4** can also recognize the Arg-Gly-Asp sequence with moderate affinity in water ($K_a = 10^3\ M^{-1}$).

Shumuck and co-workers designed guanidinocarbonylpyrrole receptor **5** possessing several hydrogen bonding sites for dipeptide binding in water (Figure 7).[26] This receptor **5**

recognizes several dipeptides through multiple hydrogen bonding in water ($K_a = 10^4\ M^{-1}$).

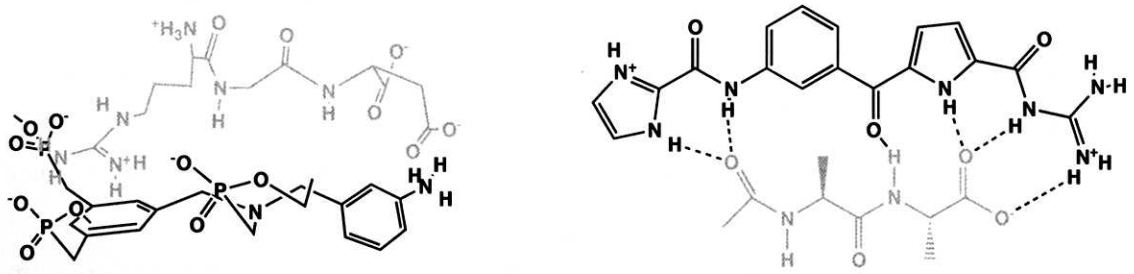

Figure 7. Chemical structures of receptor **4** synthesized by Schrader and Arg-Gly-Asp (left), and receptor **5** designed by Schmuck and Ala-Ala (right).

These receptors described above can work even in water. However, hydrogen bonding and electrostatic effect used as driving forces by their receptors are essentially unfavorable in water. In contrast, hydrophobic effect is favorable in water rather than in organic solvents.

Breslow and co-workers synthesized cyclodextrin dimer **6** (Figure 8).[27] Since cyclodextrin has a hydrophobic pocket, an aromatic side-chain of peptide is accommodated in this pocket through hydrophobic binding. Since receptor **6** has two cyclodextrin units, an oligopeptide possessing two aromatic moieties is bound by two hydrophobic interactions in water.

Quite recently, cucubit[8]uril was used by Urbach and co-workers for the selective co-recognition of an N-terminal Trp residue and methyl viologen in an aqueous solution (Figure 8).[28] This system can accommodate one electron rich aromatic ring by not only hydrophobic effect, but also charge-transfer interaction between the guest and methyl viologen in cucubit[8]uril. This system also work in water, and shows sequence-selectivity in tripeptide recognition.

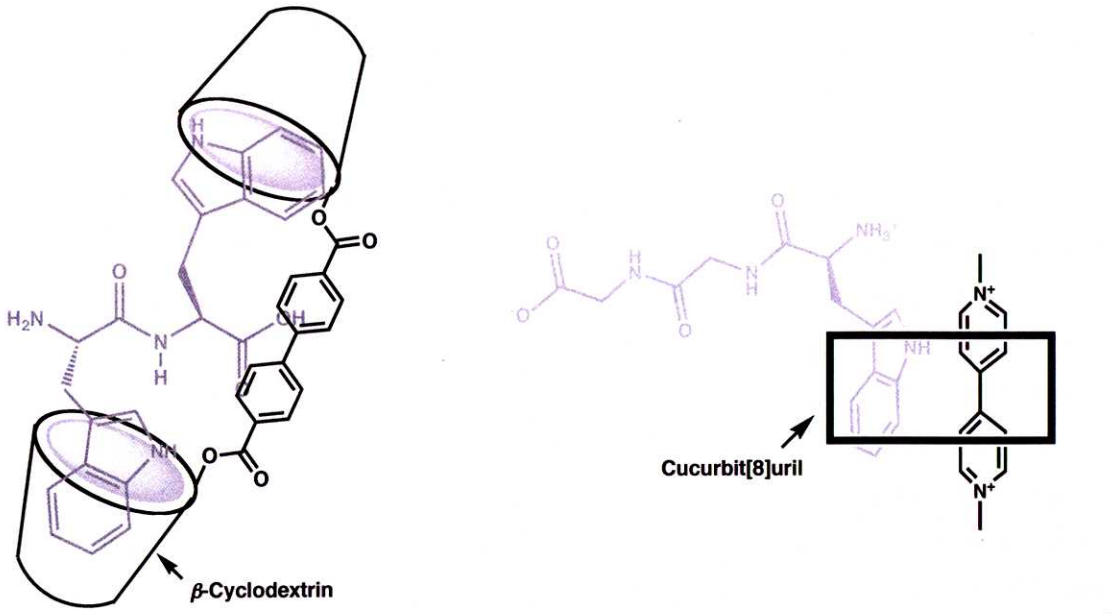

Figure 8. The chemical structure of receptor **6** binding Trp-Trp (left), and cucubit[8]uril-methyl viologen receptor system binding Trp-Gly-Gly (right).

1.3.2 Peptide receptors for the stabilization of peptide secondary structures

Most artificial peptide receptors focus on the sequence-selectivity and recognition in water. On the other hand, some receptors can stabilize the peptide secondary structures through peptide recognition. Generally, they are stabilized by cross-linking between the residues (Scheme 1).[29]

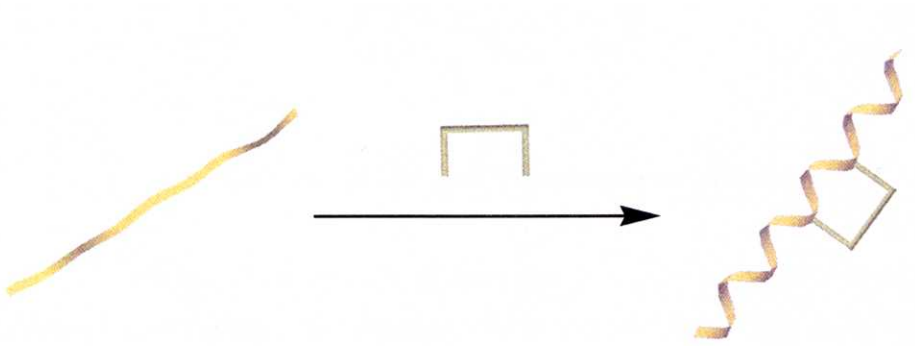

Scheme 1. Schematic representation of cross-linking between the residues for the stabilization of helical conformation.

One of the most useful strategies for the stabilization of secondary structures is recognition of basic residues, mainly His, by transition metal ions. Ghadiri and co-workers

demonstrated the stabilization of α-helical conformation by using the transition metal ions, Cu^{2+}, Zn^{2+}, Ni^{2+} and Ru^{3+}.[30] Their metal ions recognize two His residues in positions *i* and *i* + 4 of polypeptides such as Ac-Ala-Glu-Ala-Ala-Ala-Lys-Glu-Ala-Ala-Ala-Lys-***His***-Ala-Ala-Ala-***His***-Ala-NH_2. *Cis*-protected Pd^{2+} ion was also used for the stabilization of α-helical conformation by Fairlie and co-workers in a similar strategy. They used a thermolysin fragment such as Ac-***His***-Glu-Leu-Thr-***His***-Ala-Val-Thr-Asp-Tyr-NH_2 as the target sequence.[31] In contrast to His residues, phosphorylated Ser residues (pSer), concerned in some protein-protein interactions, were selectively recognized by Zn^{2+} complex receptors designed by Hamachi and co-workers.[32] In this case, the helicity of a bound peptide, Ac-Ala-Glu-Ala-Ala-Ala-Lys-Glu-Ala-***pSer***-Ala-Lys-Glu-Ala-Ala-Ala-***pSer***-Ala-NH_2, also increased via recognition of their residues.

Some sophisticated organic peptide receptors also stabilize the α-helical conformation by multiple interaction.[33] Hamilton and co-workers designed some linear peptide receptors containing multiple binding sites of amino acid side-chains. A tetraguanidinium-based receptor **7** (Figure 9) recognizes aspartate residues of peptide Ac-Ala-Ala-Ala-***Asp***-Gln-Leu-***Asp***-Ala-Leu-***Asp***-Ala-Gln-***Asp***-Ala-Ala-Tyr-NH_2 by electrostatic interaction, and its α-helical conformation is stabilized in 10% H_2O/90% MeOH.[34] This receptor **7** also recognizes Trp-rich peptide Ac-Ala-Ala-Ala-***Trp***-Gln-Leu-***Trp***-Asp-Leu-***Trp***-Asp-Ala-***Trp***-Asp-Ala-Gln-Asp-Ala-Ala-Ala-NH_2 through cation-π interaction between guanidinium moieties and the indole rings of Trp residues.[35]

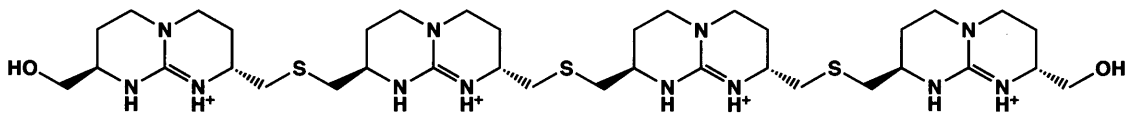

7

Figure 9. Chemical structure of receptor **7** designed by Hamilton.

A cyclodextrin dimer, similar to **6**, designed by Breslow and co-workers also showed the stabilization of α-helical structure through the hydrophobic recognition of a peptide.[36] Two cyclodextrin units bind artificial hydrophobic residues, *p-t*-butylphenylalanine (Phe'), in positions *i* and *i* + 11 of the peptide Ac-***Phe***'-Glu-Ala-Ala-Ala-Lys-Glu-Ala-Ala-Ala-Lys-***Phe***'-NH_2.

Other peptide secondary structures, β-strand and β-turn rather than α-helice, can be also stabilized by peptide receptors.[37] The stabilization of β-strand conformation was

demonstrated by Kelly and co-workers. They designed hairpin-like peptide receptors **8** composed of two peptide chain arms and dibenzofuran moiety at the middle (Figure 10).[38] A peptide fragment, R-Leu-Glu-Leu-Glu-R', is bound in between two peptide chains of **8**, forming a three-stranded β-sheet structure.

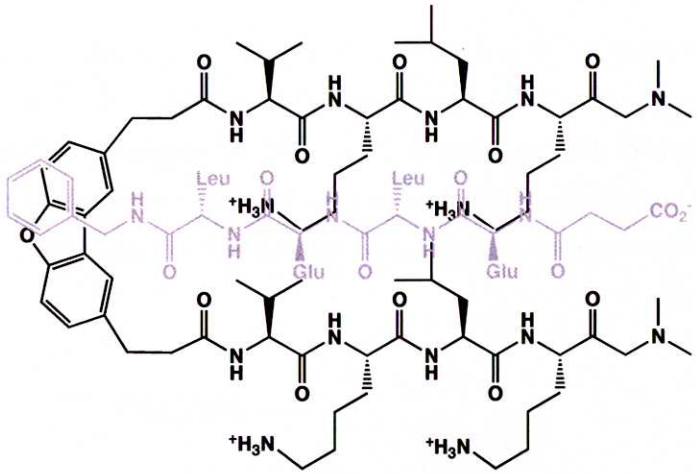

Figure 10. Chemical structures of receptor **8** designed by Kelly and β-strand guest peptide.

Veglia and co-workers demonstrated β-turn induction through the selective recognition of Cys residues.[39] They used an organotin compound for the peptide receptor. The organotin compound such as dimethyltin chloride binds two Cys residues in positions i and $i + 2$ of the peptide Ile-Leu-Gly-***Cys***-Trp-***Cys***-Tyr-Leu-Arg derived from the membrane protein stannin, and stabilized the β-turn conformation (Figure 11).

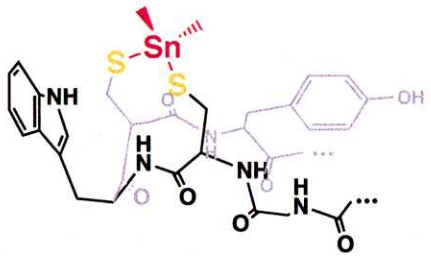

Figure 11. Chemical structure of Ile-Leu-Gly-Cys-Trp-Cys-Tyr-Leu-Arg and dimethyltin compound.

1.4 Bio-inspired Strategy for the Peptide Recognition

Generally, designed peptide receptors exhibit slight affinity in water,[40] because many artificial receptors interact with peptides through mainly hydrogen bonding. As described above, a few sophisticated receptors made it possible the moderate binding of peptides even in water ($K_a = 10^{4\sim5}\ M^{-1}$).

An ultimate example of efficient recognition is proteins as a receptor. Some proteins such as antibodies and enzymes can bind substrates very strongly ($K_a = 10^{6\sim10}\ M^{-1}$).[41] The essence of strong recognition by proteins seem to be a large and hydrophobic binding pocket on a protein surface. This pocket allows efficient hydrophobic interaction and a large number of multi-point interactions between substrates and various side chains of amino acids on protein backbones (Figure 12).

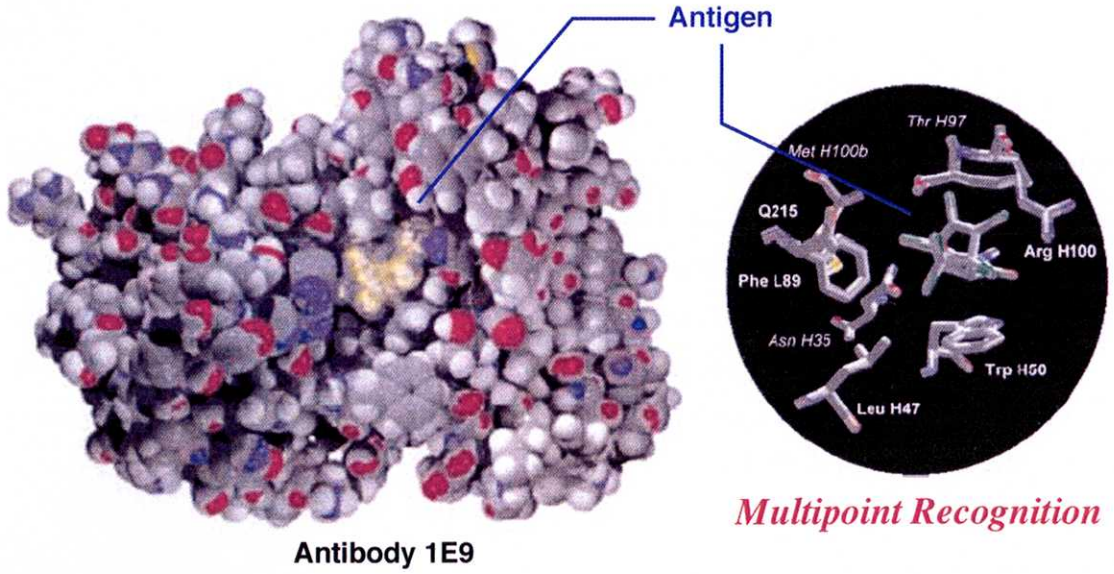

Figure 12. An example of antibody-antigen interaction. Antibody 1E9 accommodate antigen in its binding pocket. Their complex is stabilized via multipoint interaction.

The key point for strong binding in an aqueous solution and high selectivity is design of hydrophobic binding pocket, which can multiply interact with peptide. Cyclodextrin is one of superior and available receptors in terms of molecular recognition in water due to its hydrophobic cavity. As described above, some cyclodextrin derivatives have been used in amino acids and peptide recognition.[42] However, the cavity is relatively small. Thus, cyclodextrin dimers, connected by organic linkers, were synthesized for the peptide

recognition. For this reason, using the cyclodextrin derivatives seem to be limited in peptide recognition. ***Thus, the design of novel artificial receptors possessing a large hydrophobic pocket enough to bind oligopeptides is absolutely essential.***

1.5 Design of Large Hydrophobic Cavities by Self-assembly via Coordination

Fujita and co-workers have shown that nanometer-sized hollow compounds are self-assembled from simple organic ligands and transition metals in water.[43] The self-assembled hollow structure have a large hydrophobic cavity.[44] Therefore, they can accommodate moderately large organic molecules in water.

The key point of the smart self-assembly system is *cis*-protected Pd^{2+} ion, $(en)Pd(NO_3)_2$ (**9**). By the protection, the coordination number and the direction of Pd^{2+} ion are highly controlled. Therefore, the rational design of self-assembled structures become possible by combination of rigid and panel-like ligands containing pyridyl moieties. For example, 4,4'-bipyridine and **9** self-assemble into square complex **10** quantitatively in an aqueous solution (Scheme 2).[45] Furthermore, three-dimensional coordination cage **11** is self-assembled from an exo-tridentate triangular ligand, 2,4,6-tris(4-pyridyl)-1,3,5-triazine, and **9** (Scheme 3).[46] This strategy has been extended to the construction of various self-assembled hollow structures, coordination tube **12**,[47] bowl **13**,[48] and porphyrin-prism **14**[49] (Figure 13).

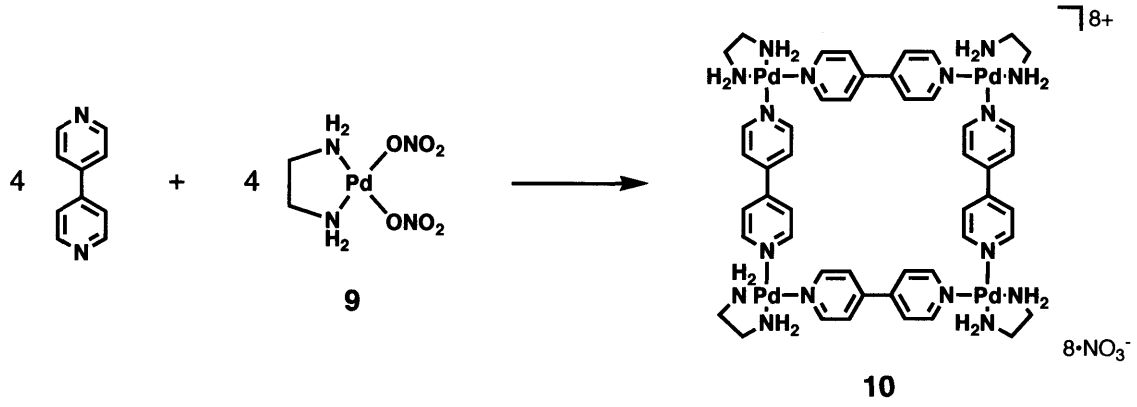

Scheme 2. Self-assembly of square complex **10**.

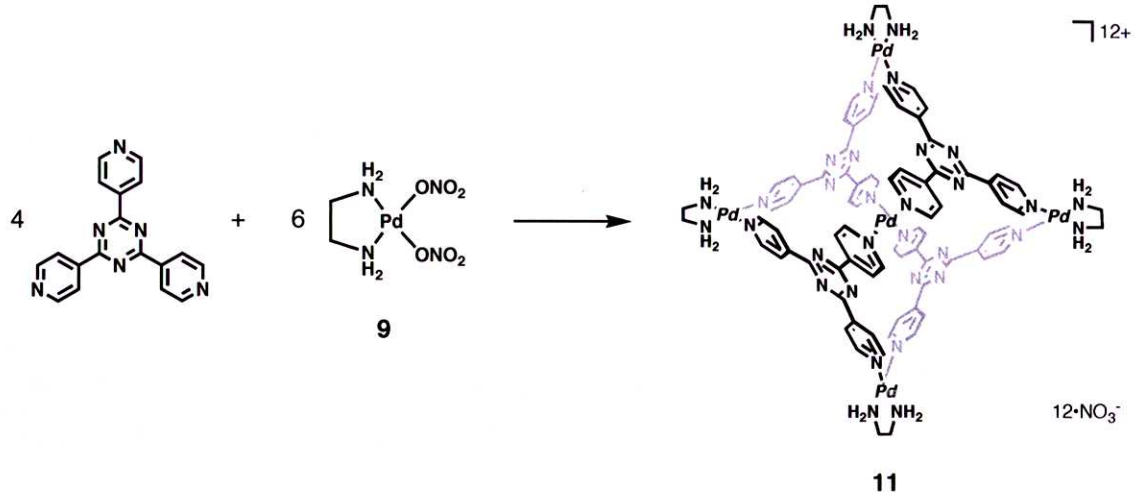

Scheme 3. Self-assembly of coordination cage **11**.

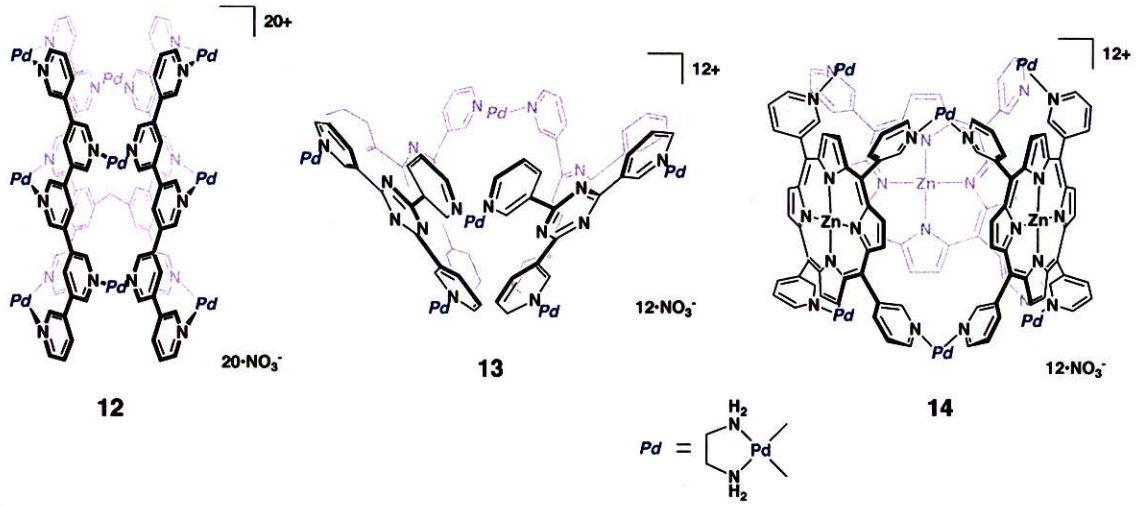

Figure 13. Chemical structures of coordination tube **12**, bowl **13** and porphyrin prism **14**.

These large hollow compounds can accommodate several organic molecules within their large hydrophobic cavity in water.[50] For example, coordination cage **11** can encapsulate four adamantane molecules in water.[51] On the other hand, coordination bowl **13** is further assembled into a dimeric capsule that accommodates as many as six neutral organic molecules.[52]

Therefore, I considered that their self-assembled coordination structures are ideal peptide receptors, because they have large hydrophobic cavities enough to fully accommodate oligopeptides in water.

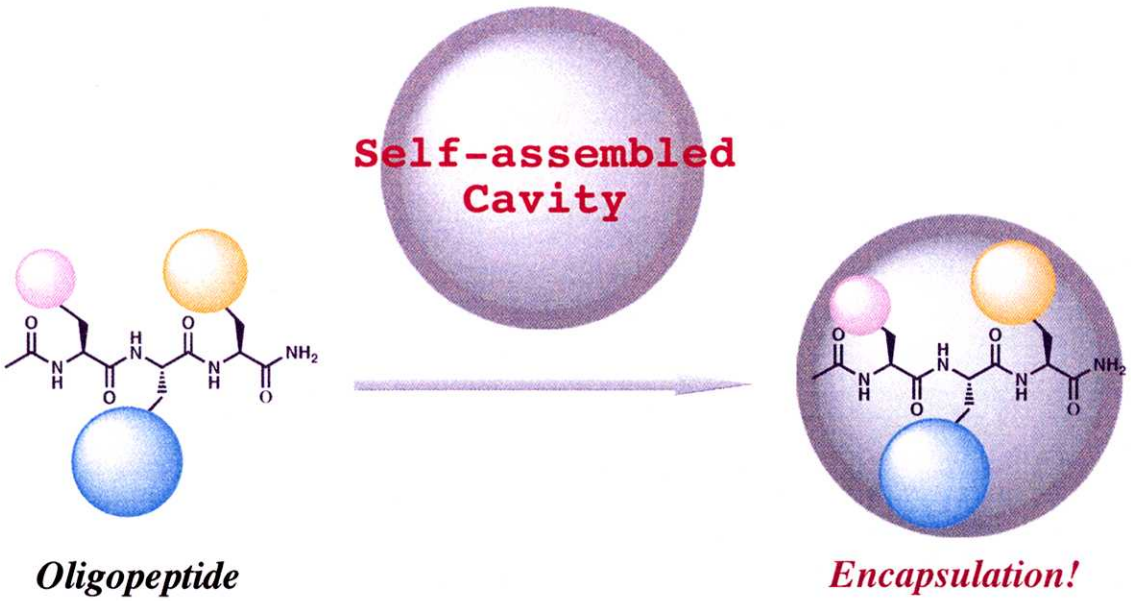

1.6 Abstracts of the Chapters

In chapter 2, the sequence-selective recognition of a tripeptide in water is described. The coordination cage **11** fully accommodates a tripeptide in a highly sequence selective fashion. In particular, Trp-Trp-Ala sequence was strongly bound in the cavity (K_a = >10^6 M^{-1}). X-ray analysis and NMR reveal that multiple interactions, CH-π and π-π interactions between the cage and Trp-Trp-Ala sequence, seem to be important in this selectivity and strong affinity. By means of the various chemical aspects of the cage, the selective recognition of several peptides was observed.

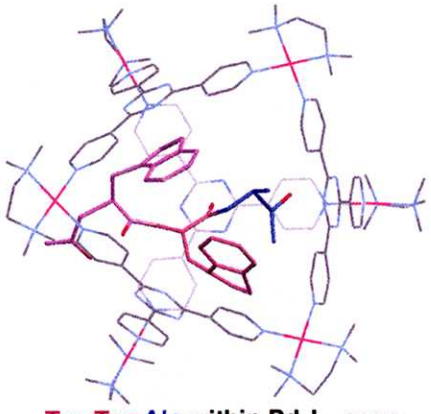

Trp-Trp-Ala within Pd_6L_4 cage

	K_a (M^{-1})
Ac-**Trp-Trp-Ala**-NH_2	>10^6
Ac-**Trp-Ala-Trp**-NH_2	2~20 x 10^4
Ac-**Ala-Trp-Trp**-NH_2	
Ac-**Trp-Trp-Gly**-NH_2	
Ac-**Trp-Tyr-Ala**-NH_2	

In chapter 3, the selective recognition of Tyr-rich peptides by using porphyrin prism complex **14** is described. The porphyrin prism showed not only high selectivity, but also very high affinity with a Tyr-Tyr sequence in water (K_a = $10^{8\sim9}$ M^{-1}). This value was comparable with that of biological recognition system such as antibody-antigen interaction. On the other hand, sequence-selectivity could be controlled by changing the porphyrin metal ions from Zn^{2+} to Au^{3+}.

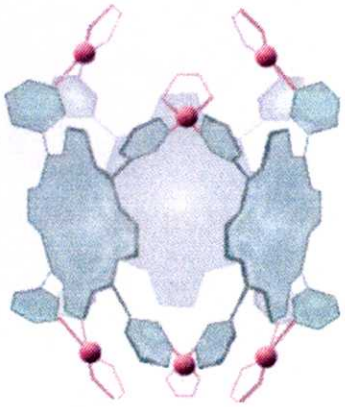

Zn(II)-porphyrin prism

High affinity & High selectivity in Water

Tyr-Tyr-Ala $K_a = 10^8\ M^{-1}$

Tyr-Ala-Tyr $K_a = 10^3\ M^{-1}$

In chapter 4, the stabilization of the α-helical conformation of a 9-residue peptide (Trp-Ala-Glu-Ala-Ala-Ala-Glu-Ala-Trp) is described. This peptide was bound in the cavity of coordination bowl **13** through hydrophobic binding in water. Although the free peptide takes random-coil conformation, the peptide forms α-helix by encapsulation within the bowl-shaped cavity. The α-helical conformation of the peptide was reliably confirmed by NOESY experiments and molecular dynamics simulation.

Bowl-shaped host

random-coil ***α-helical***

In chapter 5, the full encapsulation of a 9-residue peptide (Trp-Ala-Glu-Ala-Ala-Ala-Glu-Ala-Trp) within the dimeric capsule of coordination bowl **13** is described. The monomeric bowl sequentially recognized two Trp residues at the both terminal of the peptide through bowl/peptide = 1:1 to 2:1 complex. It was found that the formation of the 2:1 complex, where the two bowls covered the whole of the peptide, was facilitated in the presence of $NaNO_3$ due to the increase of hydrophobic interaction between Trp residues and the cavity of bowl. Furthermore, the α-helical conformation of the peptide was stabilized within the dimeric capsule of the coordination bowl.

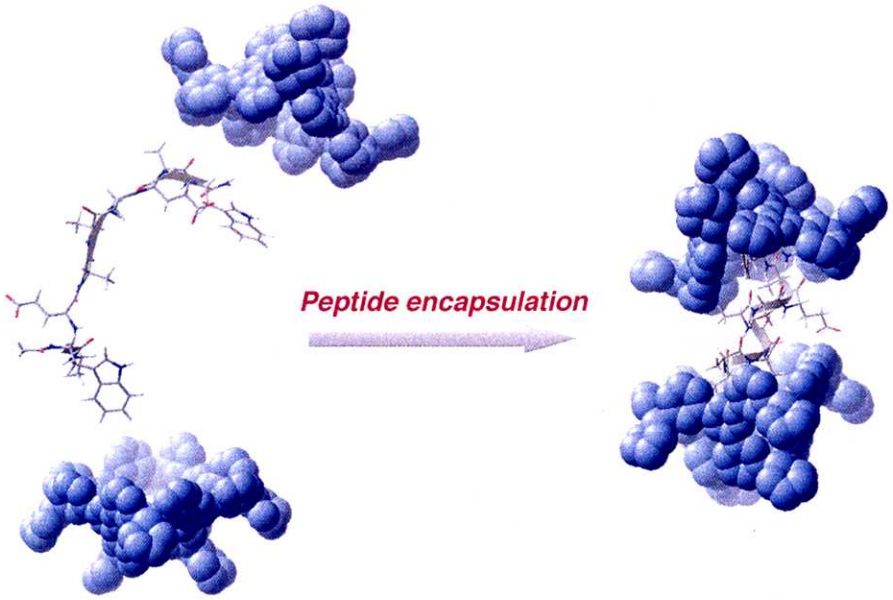

In chapter 6, the stabilization of a minimal helix, namely a β-turn structure in water is described. A tripeptide Ac-Ala-Ala-Ala-NH_2 was fully accommodated within the cavity of prophyrin prism **14**. Furthermore, this peptide folded into a turn structure within the hydrophobic cavity. The driving force of turn stabilization seemed to be multiple CH-π interaction between the methyl group of Ala residues and the porphyrin cavity.

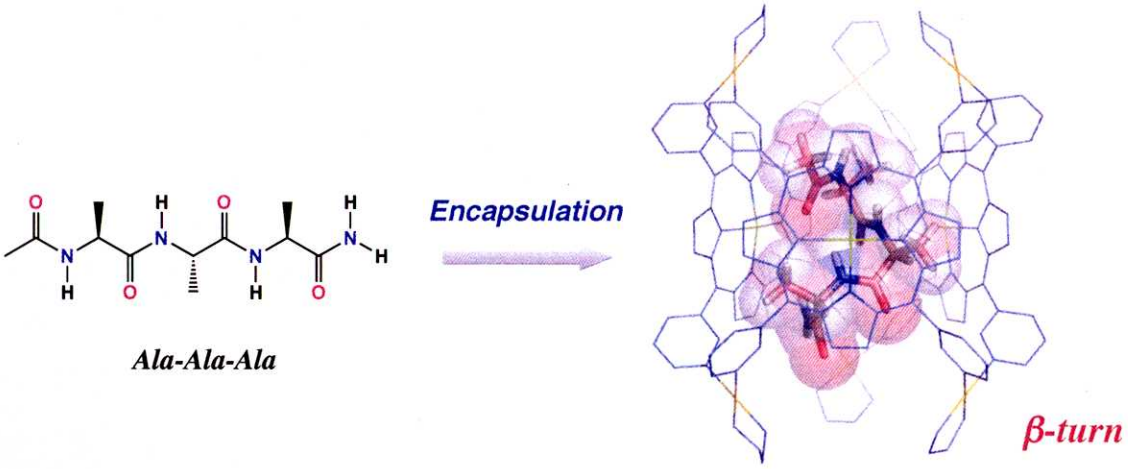

Ala-Ala-Ala

In this chapter, I advocated that there are mainly two current concerns in peptide recognition, (1) the selective recognition of peptide sequence, and (2) the control of peptide secondary structures via recognition.

Furthermore, I considered that the next challenge in peptide recognition is the design of two type of dynamic peptide receptors. As mentioned above, peptides are inherently flexible. Thus, the control of not only static peptide conformations, but also the dynamic motion of peptide chains will be needed.

On the other hand, another dynamic peptide receptor is a dynamically self-assembled host molecule. Some self-assembled structures convert to other structures by external stimuli. Namely, if the structure of peptide receptors can be regulated by external stimuli, one can control the peptide selectivity, peptide conformations in a host, and the catch/release of peptides, that is applicable to a drug delivery system, by external stimuli.

In this thesis, toward dynamic peptide receptors, I described the design of two dynamic receptors in chapter 7 and 8.

In chapter 7, toward the design of the dynamic peptide receptors, the dynamic aspect of guest molecule in coordination tube **12** is described. The motion of rod-like molecule such as biphenyl derivatives was highly restricted in the tubular cavity. Namely, rod-like guests accommodated within tube are shown to stay in the tube without flipping.

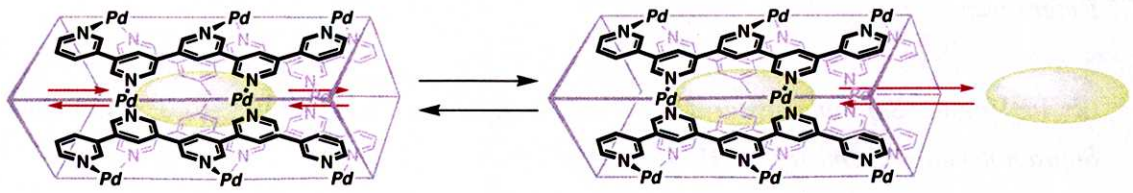

In chapter 8, toward the design of the dynamic peptide receptor, the dynamic assembly of two coordination tubes is described. Two tubes, an end-capped tube and a 3.0 nm double tube are self-assembled dynamically. At lower concentrations, only the end-capped tube was formed. On the other hand, at higher concentrations, the two tubes were self-assembled as mixture. Crystallization accelerated the structural transformation from the end-capped tube to the 3.0 nm doubly tube.

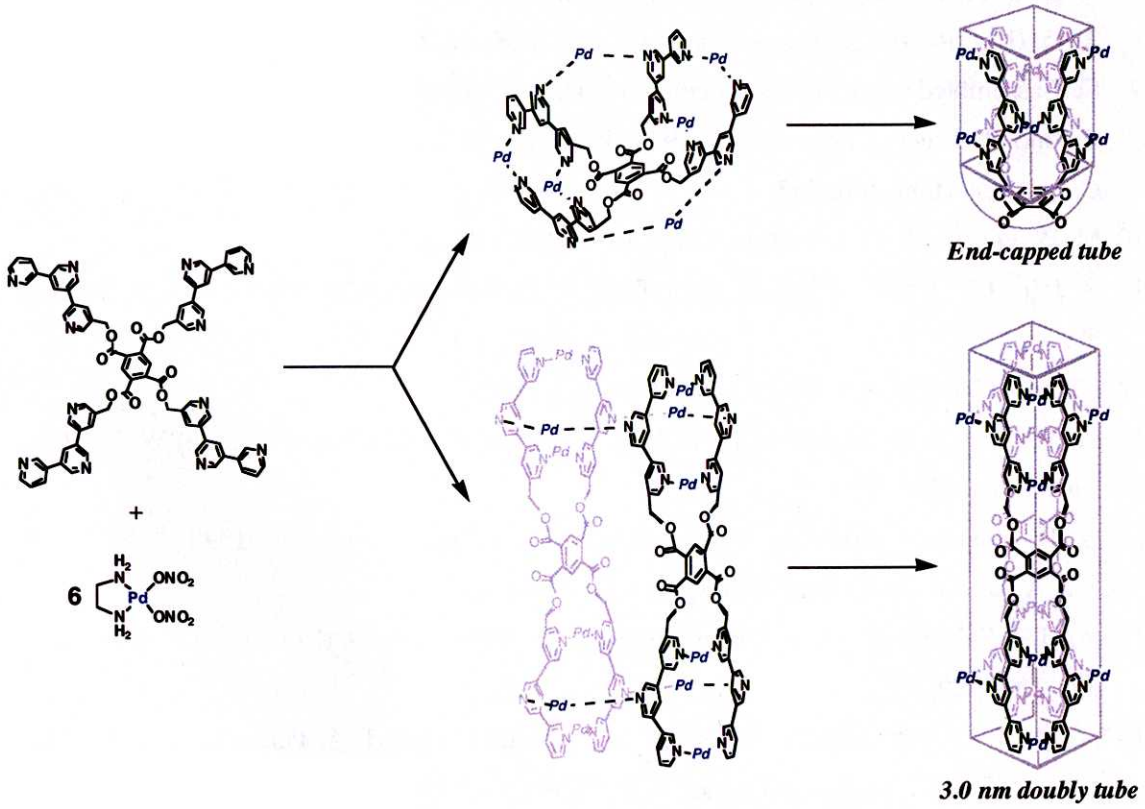

1.7 References

1 (a) F. Vögtle, *Supramolecular Chemistry,* Wiley, New York, **1991**, (b) J. M. Lehn, *Supramolecular Chemistry*, VCH, Weinheim, **1995**.

2 C. J. Pedersen, H. K. Frensdorff, *Angew. Chem. Int. Ed. Engl.* **1972**, *11*, 16.

3 J. M. Lehn, *Acc. Chem. Res.* **1978**, *11*, 49.

4 C. S. Wilcox, T. H. Webb, F. J. Zawacki, N. Glagovich, H. Suh, *Supramol. Chem.* **1993**, *1*, 129.

5 *Chem. Rev.* **1998**, *98*, 1741 (a special edition on cyclodextrins).

6 C. D. Gutsche, *Topics Curr. Chem.* **1984**, *123*, 1.

7 R. Warmuth, *J. Chem. Soc., Chem. Commun*, **1998**, 59.

8 Self-assembled hosts via hydrogen bond: (a) P. Timmerman, W. Verboom, F. C. J. M. van Veggel, J. P. M. van Duynhoven, D. N. Reinhoudt, *Angew. Chem. Int. Ed. Engl.* **1994**, *33*, 2345. (b) J. Rebek, Jr. *Angew. Chem. Int. Ed.* **2005**, *44*, 2068.

9 Self-assembled hosts via coordination: (a) D. L. Caulder, R. E. Powers, T. N. Parac, K. N. Raymond, *Angew. Chem. Int. Ed.* **1998**, *37*, 1840. (b) S. Leininger, B. Olenyuk, P. J. Stang, *Chem. Rev.* **2000**, *100*, 853.

10 M. W. Peczuh, A. D. Hamilton, *Chem. Rev.* **2000**, *100*, 2479.

11 R. Jain, J. T. Ernst, O. Kutzki, H. S. Park, A. D. Hamilton, *Molecular Diversity,* **2004**, *8*, 89.

12 J. Janin, C. Chothia, *J. Biol. Chem.* **1990**, *265*, 16027.

13 (a) S. Jones, J. M. Thornton, *Proc. Natl. Acad. Sci. U.S.A.* **1996**, *93*, 13. (b) W. E. Stites, *Chem. Rev.* **1997**, *97*, 1233.

14 (a) R. Zutshi, M. Brickner, J. Chmielewski, *Curr. Opin. Chem. Biol.* **1998**, *2*, 62. (b) H. Yin, A. D. Hamilton, *Angew. Chem. Int. Ed.* **2005**, *44*, 4130.

15 (a) H.-J. Schneider, *Angew. Chem. Int. Ed. Engl.* **1993**, *32*, 848. (b) W. C. Still, *Acc. Chem. Res.* **1996**, *29*, 155.

16 (a) M. D. Pierschbacher, E. Ruoslathi, J. Sundelin, P. Lind, P. A. Peterson, *J. Biol. Chem.* **1982**, *257*, 9593. (b) J. M. Gardner, R. O. Hynes, *Cell* **1985**, *42*, 439.

17 L. O. Tjernberg, J. Näslund, F. Lindqvist, J. Johansson, A. R. Karlström, J. Thyberg, L. Terenius, C. Nordstedt, *J. Biol. Chem.* **1996**, *271*, 8545.

18 D. H. Williams, *Acc. Chem. Res.* **1984**, *17*, 364.

19 M. G. Rossmann, P. Argos, *Annu. Rev. Biochem.* **1981**, *50*, 497.

20 (a) P. D. Henley, J. D. Kilburn, *Chem. Commun.* **1999**, 1335. (b) K. Tsubaki, T. Kusumoto, N. Hayashi, M. Nuruzzaman, K. Fuji, *Org. Lett.* **2002**, *4*, 2313.

21 (a) J.-I. Hong, S. K. Namgoong, A. Bernardi, W. C. Still, *J. Am. Chem. Soc.* **1991**, *113*, 5111. (b) S. S. Yoon, W. C. Still, *Angew. Chem. Int. Ed. Engl.* **1994**, *33*, 2458.

22 (a) C. Schmuck, *Chem. Commun.* **1999**, 843. (b) S. Sun, M. A. Fazal, B. C. Roy, S. Mallik, *Org. Lett.* **2000**, *2*, 911. (c) T. Mizutani, K. Wada, S. Kitagawa, *Chem. Commun.* **2002**, 1626. (d) A. T. Wright, E. V. Anslyn, *Org. Lett.* **2004**, *6*, 1341.

23 M. A. Hossain, H.-J. Schneider, *J. Am. Chem. Soc.* **1998**, *120*, 11208.

24 M. Sirish, H.-J. Schneider, *Chem. Commun.* **1999**, 907.

25 S. Rensing, T. Schrader, *Org. Lett.* **2002**, 4, 2161.

26 C. Schmuck, L. Geiger, *J. Am. Chem. Soc.* **2004**, *126*, 8898.

27 R. Breslow, Z. Yang, R. Ching, G. Trojandt, F. Odobel, *J. Am. Chem. Soc.* **1998**, *120*, 3536.

28 M. E. Bush, N. D. Bouley, A. R. Urbach, *J. Am. Chem. Soc.* **2005**, *127*, 14511.

29 J. P. Schneider, J. W. Kelly, *Chem. Rev.* **1995**, *95*, 2169.

30 (a) M. R. Ghadiri, C. Choi, *J. Am. Chem. Soc.* **1990**, *112*, 1630. (b) M. R. Ghadiri, A. K. Fernholz, *J. Am. Chem. Soc.* **1990**, *112*, 9633.

31 (a) M. J. Kelso, H. N. Hoang, W. Oliver, N. Sokolenko, D. R. March, T. G. Appleton, D. P. Fairlie, *Angew. Chem. Int. Ed.* **2003**, *42*, 421. (b) M. J. Kelso, R. L. Beyer, H. N. Hoang, A. S. Lakdawala, J. P. Snyder, W. V. Oliver, T. A. Robertson, T. G. Appleton, D. P. Fairlie, *J. Am. Chem. Soc.* **2004**, *126*, 4828.

32 A. Ojida, M. Inoue, Y. Mito-oka, I. Hamachi, *J. Am. Chem. Soc.* **2003**, *125*, 10184.

33 (a) D. J. Cline, C. Thorpe, J. P. Schneider, *J. Am. Chem. Soc.* **2003**, *125*, 2923. (b) A. Verma, H. Nakade, J. M. Simard, V. M. Rotello, *J. Am. Chem. Soc.* **2004**, *126*, 10806.

34 M. W. Peczuh, A. D. Hamilton, J. Sánchez-Quesada, J. de Mendoza, T. Haack, E. Giralt, *J. Am. Chem. Soc.* **1997**, *119*, 9327.

35 B. P. Orner, X. Salvatella, J. Sánchez-Quesada, J. de Mendoza, E. Giralt, A. D. Hamilton, *Angew. Chem. Int. Ed.* **2002**, *41*, 117.

36 D. Wilson, L. Perlson, R. Breslow, *Bioorg. Med. Chem.* **2003**, *11*, 2649.

37 (a) C. N. Kirsten, T. H. Schrader, *J. Am. Chem. Soc.* **1997**, *119*, 12061. (b) K. Ryan, L. J. Gershell, W. C. Still, *Tetrahedron*, **2000**, *56*, 3309. (c) P. Pzepecki, T. Schrader, *J. Am. Chem. Soc.* **2005**, *127*, 3016.

38 S. R. LaBrenz, J. W. Kelly, *J. Am. Chem. Soc.* **1995**, *117*, 1655.

39 B. A. Buck, A. Mascioni, C. J. Cramer, G. Veglia, *J. Am. Chem. Soc.* **2004**, *126*, 14400.

40 R. M. Izatt, J. S. Bradshaw, K. Pawlak, R. L. Bruening, B. J. Tarbet, *Chem. Rev.* **1992**, *92*, 1261.

41 K. N. Houk, A. G. Leach, S. P. Kim, X. Zhang, *Angew. Chem. Int. Ed.* **2003**, *42*, 4872.

42 (a) R. Breslow, B. Zhang, *J. Am. Chem. Soc.* **1992**, *114*, 5882. (b) R. Ueoka, Y. Matsumoto, K. Harada, H. Akahoshi, Y. Ihara, Y. Kato, *J. Am. Chem. Soc.* **1992**, *114*, 8339.

43 (a) M. Fujita, *Chem. Soc. Rev.* **1998**, *27*, 417. (b) M. Fujita, K. Umemoto, M. Yoshizawa, N. Fujita, T. Kusukawa, K. Biradha, *Chem. Commun.* **2001**, 509. (c) M. Fujita, M. Tominaga, A. Hori, B. Therrien, *Acc. Chem. Res.* **2005**, *38*, 371.

44 (a) N. Takeda, K. Umemoto, K. Yamaguchi, M. Fujita, *Nature*, **1999**, *398*, 794. (b) Y. Yamanoi, Y. Sakamoto, T. Kusukawa, M. Fujita, S. Sakamoto, K. Yamaguchi, *J. Am. Chem. Soc.* **2001**, *123*, 980. (c) J.-P. Bourgeois, M. Fujita, M. Kawano, S. Sakamoto, K. Yamaguchi, *J. Am. Chem. Soc.* **2003**, *125*, 9260. (d) M. Tominaga, K. Suzuki, M. Kawano, T. Kusukawa, T. Ozeki, S. Sakamoto, K. Yamaguchi, M. Fujita, *Angew. Chem. Int. Ed.* **2004**, *43*, 5621. (e) M. Yoshizawa, J. Nakagawa, K. Kumazawa, M. Nagao, M. Kawano, T. Ozeki, M. Fujita, *Angew. Chem. Int. Ed.* **2005**, *44*, 1810.

45 M. Fujita, J. Yazaki, K. Ogura, *J. Am. Chem. Soc.* **1990**, *112*, 5645.

46 M. Fujita, D. Oguro, M. Miyazawa, H. Oka, K. Yamaguchi, K. Ogura, *Nature*, **1995**, *378*, 469.

47 M. Aoyagi, K. Biradha, M. Fujita, *J. Am. Chem. Soc.* **1999**, *121*, 7457.

48 M. Fujita, S.-Y. Yu, T. Kusukawa, H. Funaki, K. Ogura, K. Yamaguchi, *Angew. Chem. Int. Ed.* **1998**, *37*, 2082.

49 N. Fujita, K. Biradha, M. Fujita, S. Sakamoto, K. Yamaguchi, *Angew. Chem. Int. Ed.* **2001**, *40*, 1718.

50 (a) T. Kusukawa, M. Fujita, *J. Am. Chem. Soc.* **2002**, *124*, 13576. (b) M. Yoshizawa, M. Tamura, M. Fujita, *J. Am. Chem. Soc.* **2004**, *126*, 6846.

51 T. Kusukawa, M. Fujita, *Angew. Chem. Int. Ed.* **1998**, *37*, 3142.

52 S.-Y. Yu, T. Kusukawa, K. Biradha, M. Fujita, *J. Am. Chem. Soc.* **2000**, *122*, 2665.

Chapter 2

Sequence-selective Recognition of Tri-peptides within Coordination Cages

Abstract

The single binding pocket of a self-assembled Pd_6L_4 coordination cage recognizes oligopeptides in a highly sequence selective fashion. In particular, the Trp-Trp-Ala sequence is strongly bound by the cavity (K_a = >10^6 M^{-1}). Tripeptides possessing the same residues but in different sequences (i.e., Trp-Ala-Trp and Ala-Trp-Trp) show much poorer affinity. Even singly mutated tripeptides with aromatic-aromatic-aliphatic sequences of the residues (e.g., Trp-Trp-Gly and Trp-Tyr-Ala) are not recognized efficiently. X-ray analysis and NMR reveal that all residues of the Trp-Trp-Ala sequence cooperatively interact with the cage via CH-π and π-π interactions.

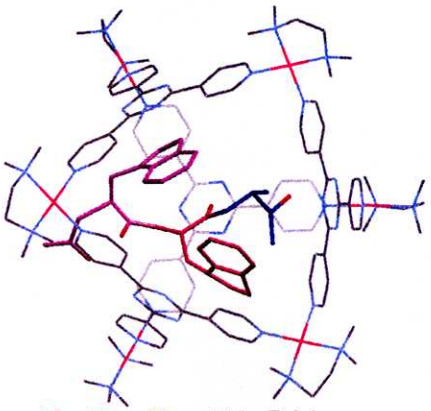

Trp-Trp-Ala within Pd_6L_4 cage

	K_a (M^{-1})
Ac-**Trp-Trp-Ala**-NH_2	>10^6
Ac-**Trp-Ala-Trp**-NH_2	2~20 x 10^4
Ac-**Ala-Trp-Trp**-NH_2	
Ac-**Trp-Trp-Gly**-NH_2	
Ac-**Trp-Tyr-Ala**-NH_2	

2.1 Introduction

Peptide recognition is an essential process in biological events, such as protein-protein interaction, hormone-receptor interaction, and cell-cell adhesion.[1] In the peptide recognition by synthetic receptors, it is particularly important to recognize the sequence of peptides because the sequence-selective peptide recognition can be applied to the site-specific recognition of protein surface, which lead to the control of protein-protein and protein-substrate interactions.[2] Recently, for the site-specific recognition of protein surface, a number of artificial peptide receptors were designed. In general, the sequence-selective recognition of oligopeptides is accomplished by linking two or more binding sites of synthetic receptors.[3] An interesting example is Hamilton's well-designed receptors that recognize peptide secondary structures such as α-helix as well as a protein surface.[4]

It is known that protein surfaces mediating protein-protein interactions are abundant in aromatic residues such as Tyr and Trp.[5] Those aromatic residues are especially localized in antigen binding sites of antibodies, which are called complementarity determining regions (CDR).[6] Thus, sequence-selective recognition of aromatic residues is particularly important to control the protein surface interactions. Cyclodextrin, which is one of the useful aromatic peptide receptors, can bind only one aromatic side chain within its relatively small cavity. For aromatic oligopeptide recognition, two or more cyclodextrins should be linked by covalent bonds.[7]

Here, we report the single binding pocket of self-assembled coordination cages[8] **1** and **1'** can accommodate oligopeptides in a highly sequence-selective fashion. Having a large hydrophobic cavity, cages bind as many as three amino acid residues. NMR and X-ray analyses reveal that the sequence-selective recognition is ascribed to cooperative multiple interactions between the residues and the cavity. Furthermore, cages discriminated charged residues in peptide by using the highly cationic property of cages.

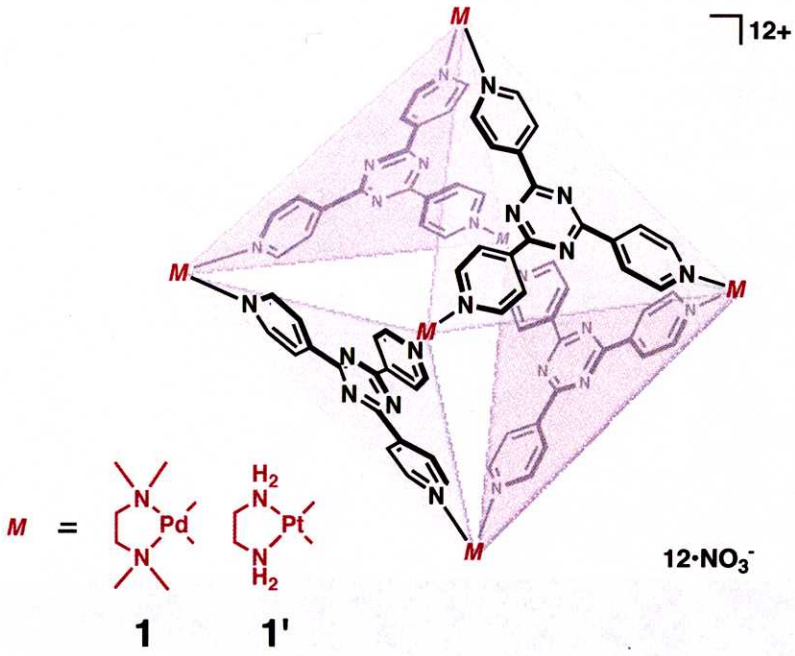

2.2 *Result and Discussion*

2.2.1 Association constants between cage **1** and peptides in water

In a first series, the sequence selective recognition of tripeptides, Ac-X^1-X^2-X^3-NH_2 ($X^{1\text{-}3}$ = amino acid residues), was examined.[9] The complexes of cage **1** and peptides were easily prepared by mixing of both solutions at room temperature for a few minutes. Association constants of those peptides were measured by the UV titration in water. We found that cage **1** bound Ac-Trp-Trp-Ala-NH_2 (**2**) very strongly ($K_a > 10^6$ M^{-1}).[10] Strong binding was specific to the Trp-Trp-Ala sequence because the binding of tripeptides possessing those same residues in different sequences, such as Ac-Trp-Ala-Trp-NH_2 (**3**) and Ac-Ala-Trp-Trp-NH_2 (**4**), was much less effective (K_a = 2.5 x 10^5 and 2.1 x 10^4 M^{-1}, respectively). Even singly mutated tripeptides, such as Ac-Trp-Trp-Gly-NH_2 (**5**) and Ac-Trp-Tyr-Ala-NH_2 (**6**), showed poorer affinity (K_a = 7.4 x 10^4 and 5.3 x 10^4 M^{-1}, respectively) though they have very similar aromatic-aromatic-aliphatic sequences (Table 1). These results suggest that the two indole rings and the Ala methyl group in **2** should cooperatively interact with the cage in the **1•2** complex.

Table 1. Association constants of **1** with tripeptides in water

Peptides	K_a (M^{-1})[a]
Ac-**Trp-Trp-**Ala-NH_2 (**2**)	$>10^6$
Ac-**Trp-**Ala-**Trp-**NH_2 (**3**)	2.5 (± 0.8) x 10^5
Ac-Ala-**Trp-Trp-**NH_2 (**4**)	2.1 (± 0.2) x 10^4
Ac-**Trp-Trp-**Gly-NH_2 (**5**)	7.4 (± 4.6) x 10^4
Ac-**Trp-**Tyr-Ala-NH_2 (**6**)	5.3 (± 2.3) x 10^4

[a] Measured by UV-vis titration at 20 °C.

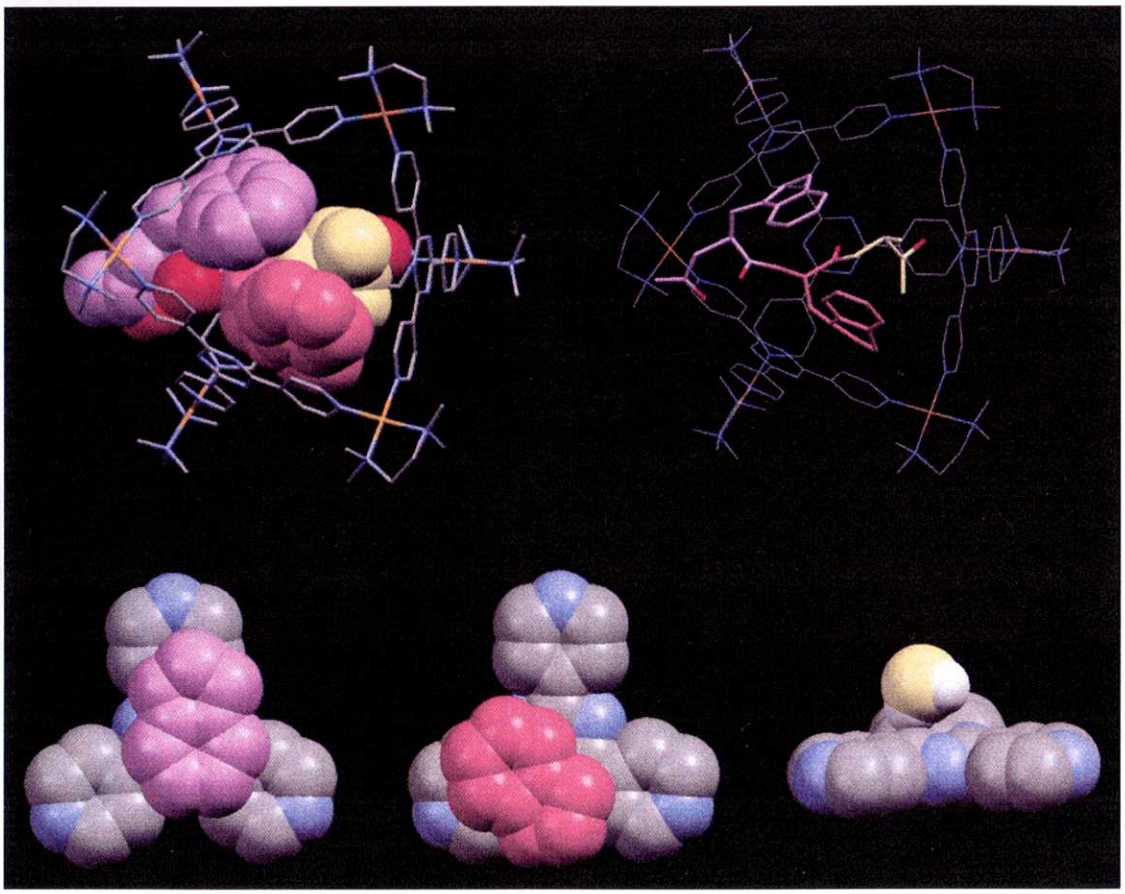

Figure 1. Crystal structure of **1•2**. Peptide **2** in the cavity is represented by (a) space-filling and (b) cylindrical model. The π-π interactions of **1** with indole rings of (c) W1 and (d) W2. (e) The CH-π interaction between **1** and methyl group of A3.

2.2.2 X-ray crystallographic analysis of inclusion complex **1•2**

The multiple interactions of the methyl and indole groups with the cage were revealed by X-ray crystallographic analysis. Single crystals were obtained by standing an aqueous solution of **1•2** complex at room temperature for 4 d. The diffraction data were collected by synchrotron X-ray irradiation. The crystallographic analysis showed that tripeptide **2** is fully encapsulated in the cavity of **1** (Figure 1a,b). As predicted, all residues interact very efficiently with cage **1**. Namely, two indole rings are stacked on the triazine ligand by π-π interaction (3.4-3.5 Å), while the Ala methyl group interacts with another ligand by CH-π contact (2.5 Å) (Figure 1c-e). Despite the enclathration within the restricted cavity, the peptide backbone is fixed in an extended conformation.

2.2.3 NMR analysis of inclusion complex **1•2**

The inclusion geometry shown by the X-ray analysis is in good agreement with the NMR observations. In the ^{1}H NMR, the Ala methyl signal at δ –2.0 and the indole aromatic protons around δ 6.0-2.5 are considerably upfield shifted due to the shielding effect of the cage (Figure 2). A clear NOE correlation between the Ala methyl group (signal *q* in Figure 2) and one indole ring (signal *e*) was observed, which was explained by the tight contact of these proton pairs (2.6 Å) as revealed by X-ray analysis. Similarly, two indole rings (signals *g* and *n*) are correlated by NOE and shown to be in close contact (2.8 Å). In the δ 10.0-8.0 region, the pyridyl protons of the cage were observed in a very complex pattern indicating the desymmetrization of the cage. The motion of **2** is restricted by enclathration and therefore all pyridine protons of the cage become inequivalent. We note that the clear desymmetrization of the cage in NMR is only observed for **2**. It seems that the motions of other tripeptides in the cavity are not strictly restricted and, therefore, the ^{1}H NMR cage signals are simply broadened.

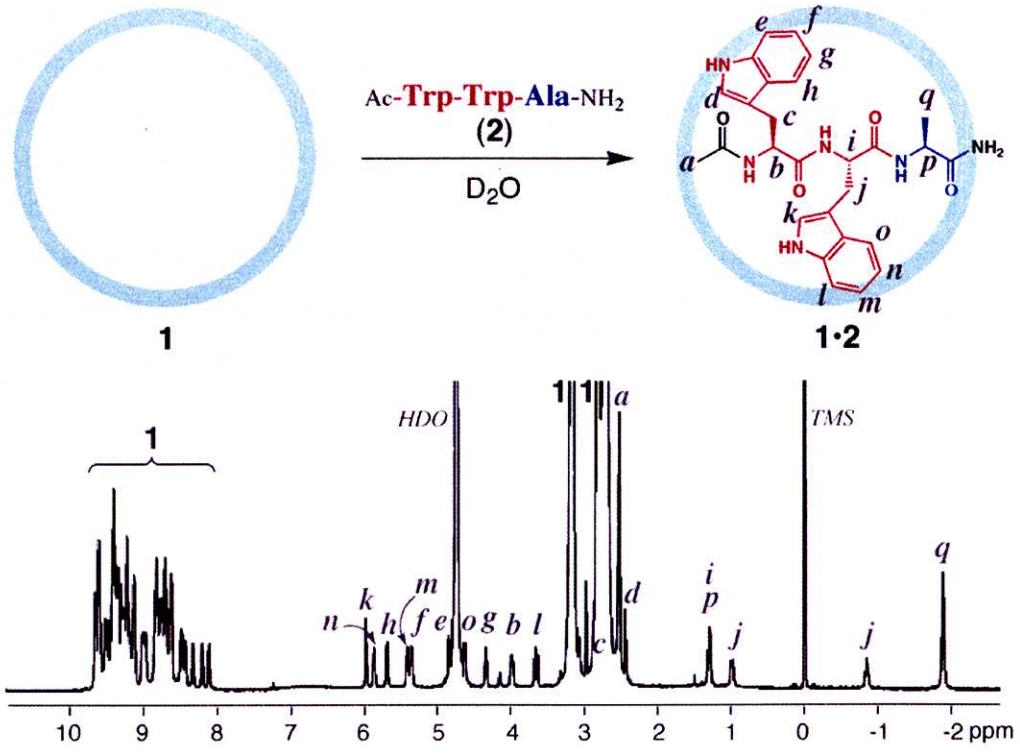

Figure 2. ^{1}H NMR of **1•2** in D_2O (500 MHz, 10 mM, 27 °C, TMS as external standard).

2.2.4 Charge transfer interaction between cage **1** and indole ring of tryptophan residues

The efficient π-π stacking observed by X-ray and NMR is ascribed to charge transfer from the indole rings to the electron deficient triazine ligand.[11] The color of the solution turned yellow upon formation of the **1•2** complex. In the UV-vis spectrum, broad absorption around 350-550 nm was observed (Figure 3).

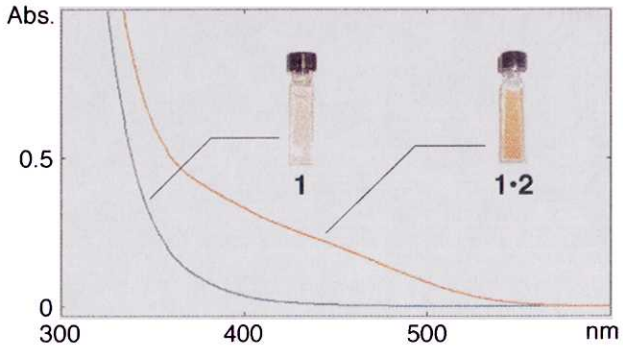

Figure 3. UV-vis spectra of free cage **1** and complex **1•2** (H_2O, 0.2 mM, rt).

2.2.5 Sequence-selectivity of tryptophan and tyrsine residues within cage

Coordination cage could discriminate similar aromatic residues, even Trp and Tyr in oligopeptides, by charge-transfer interaction between electron-rich aromatic residues and electron-deficient triazine parts of the cage. In this case, the platinum cage **1'** was used instead of palladium cage **1**, because the platinum cage **1** has substantial stability for basic and acidic conditions compared with acid and base labile palladium cage **1'**. The Trp-rich peptide Ac-Ala-Trp-Trp-NH_2 (**4**) was bound about 5-fold stronger than Ac-Ala-Tyr-Tyr-NH_2 (**7**) in acetate buffer solution (Table 2). This difference is attributed to efficiency of charge-transfer interactions, because complex **1'•4** has more red-shifted charge-transfer absorption than **1'•7** (Figure 4).

Table 2. Association constants of **1'** with peptides in water

Peptides	K_a (M^{-1})[a]	
	pH 4.8 (Acetate buffer)	pH 9.0 (Borate buffer)
Ac-Ala-**Trp-Trp**-NH_2 (**4**)	3.7 (± 0.6) x 10^4	4.0 (± 0.2) x 10^4
Ac-Ala-Tyr-Tyr-NH_2 (**7**)	6.8 (± 1.2) x 10^3	> 10^5

[a] Measured by UV-vis titration at 20 °C in 5 mM buffer solution.

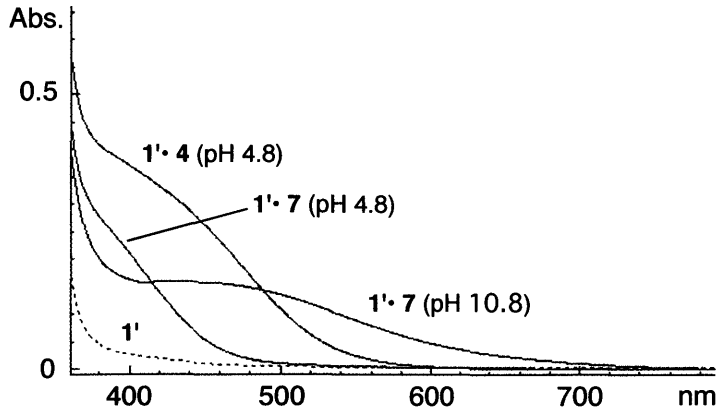

Figure 4. UV spectra of **1'**, **1'•4** (pH 4.8) and **1'•7** (pH 4.8 and 10.8) at 20 °C ([**1'**], [**4**] and [**7**] = 3.0 mM in H_2O).

Interestingly, selectivity of aromatic peptides having Trp and Tyr residues was reversed in basic condition. In borate buffer solution (pH 9.0), peptide **7** was bound about ten times as strong as **4**, whose affinity with **1'** showed little difference in any pH conditions (Table 2). Since the charge-transfer band of **1'•7** in basic condition were more red-shifted than that of acidic condition, increment of binding constant of **1'•7** was ascribed to not only electrostatic

attraction but also efficient charge-transfer interaction between phenolate anion of Tyr residues and cage **1'** (Figure 4).

This behavior was applicable to naked-eye recognition of colorless aromatic peptides. The Trp residues in peptides were detected from coloring of peptide solution by addition of **1'**. For example, solution of the **1'•4** complex showed orange color in any pH condition. Interestingly, cage **1'** could discriminate Trp and Tyr residues even in naked-eye recognition. While the solution of complex **1'•7** showed pale yellow in acidic or neutral conditions, solution color changed into red in basic condition (Figure 5). This color change corresponds with change of UV spectra as shown in Figure 4. On the other hand, Phe residues in peptides exhibited little color change in the presence of cage **1'**. Namely, we could discriminate three aromatic residues, Trp. Tyr and Phe from solution colors by mixing of coordination cage **1'**. Of course, this behavior was observed in the case of not only peptides but also just amino acids.

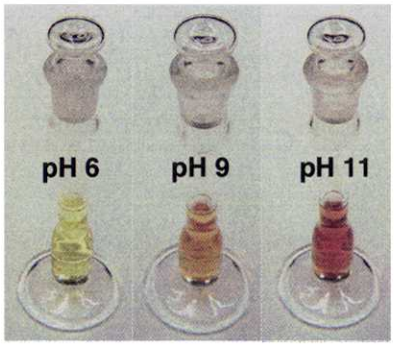

Figure 5. Pictures of **1'•7** solution under several pH conditions ([**1'**] and [**7**] = 3.0 mM in H_2O). The solution was adjusted from pH 6 to pH 11 using 100 mM NaOH.

2.2.6 Selective and site-specific recognition of hexapeptides

We examined selective recognition of not only tripeptides, but also longer peptides by using the steric effect of cage **1'**. Hexapeptide, Ac-Ser-Gly-Ala-Trp-Trp-Ala-NH_2 (**8**) possessing additional Ser-Gly-Ala sequence from N-terminal of **2**, was bound in **1'** with high affinity (K_a > 10^5 M^{-1}). However, Ac-Ala-Trp-Trp-Ala-Gly-Ser-NH_2 (**9**), having additional sequences at both terminal of **2**, showed poorer affinity than **8** (K_a = 7.2 x 10^4 M^{-1}). Namely, cage **1'** could discriminate similar two hexapeptides, possessing those same residues in different sequences and Trp-Trp-Ala sequence each other (Table 3). This selectivity is explained by disturbing the stable conformation of **1'•2** from steric repulsion between cage and elongated sequence from C-terminal. From crystal structure of complex **1•2**, C-terminal of **2** is inside of cavity compared to N-terminal, which is outside of cavity (Figure 1). This results imply

that cage can recognize the long polypeptide chain with high affinity (> 10^5 M^{-1}), if peptide has Trp-Trp-Ala sequence at C-terminal such as peptide **8**.

Furthermore, the cage discriminated charged peptides by electrostatic attraction and repulsion in various pH, because of highly cationic property of the cage (12+). We elucidated electrostatic effect by using hexapeptide Ac-Ala-Trp-Trp-Ala-Gly-Xxx-NH_2. In acidic condition, the association constant of **1'** with hexapeptide Ac-Ala-Trp-Trp-Ala-Gly-Lys-NH_2 (**10**), possessing cationic residue Lys, was dramatically decreasing (Table 3). On the other hand, anionic peptide Ac-Ala-Trp-Trp-Ala-Gly-Glu-NH_2 (**11**) showed higher affinity than neutral peptide **9** in any pH conditions. This suggests that cage **1'** prefers anionic and neutral peptides to cationic peptides more than 100-fold in acidic condition.

Table 3. Association constants of **1'** with peptides in water

Peptides	K_a (M^{-1})[a]	
	pH 4.8 (Acetate buffer)	pH 9.0 (Borate buffer)
Ac-Ser-Gly-Ala-**Trp-Trp-**Ala-NH_2 (**8**)	> 10^5	-
Ac-Ala-**Trp-Trp-**Ala-Gly-Ser-NH_2 (**9**)	7.2 (± 1.9) x 10^4	9.5 (± 1.5) x 10^4
Ac-Ala-**Trp-Trp-**Ala-Gly-Lys-NH_2 (**10**)	< 10^3	2.0 (± 0.3) x 10^4
Ac-Ala-**Trp-Trp-**Ala-Gly-Glu-NH_2 (**11**)	2.4 (± 0.4) x 10^5[b]	> 10^6

[a] Measured by UV-vis titration at 20 °C in 5 mM buffer solution.

[b] Measured in 5 mM phosphate buffer solution (pH 2.6).

2.3 Conclusion

In conclusion, we have shown the sequence-selective recognition of peptides by the single binding pocket of cage **1**. Among the various tripeptides, Trp-Trp-Ala sequence was bound very strongly. The X-ray analysis of **1•2** revealed that sequence-selectivity was explained from cooperatively multiple-interaction between triazine-core of **1** and indole rings of **2**. This behavior seemed to be maintained even in solution from NMR measurements and coloring of the solution by charge-transfer interaction between **1** and **2**. The charge-transfer interaction was also applicable to recognition and naked-eye detection of aromatic residues. Furthermore, cage **1** could discriminate some longer hexa-peptides from steric repulsion and electrostatic interaction.

As organic modification of the cage is easy, and related large hollow structures with different shapes and sizes have been previously prepared,[12] the design of single pocket

receptors for specific sequences of oligopeptides is our next challenge. Ultimately, the pinpoint recognition of protein surfaces by these self-assembled hollow receptors is the main goal of the present study.

2.4 Experimental Section

Materials, peptide synthesis, procedure of UV titration and NMR measurements were described in General Experimental Section. Coordination cages **1** and **1'** were prepared following procedure as reported earlier.[8,13]

Physical data of 1•2

^{1}H NMR (500 MHz, D_2O, 27 °C, TMS as external standard): δ 9.67 (d, J = 5.0 Hz, 2H, **1**), δ 9.63 (m, 4H, **1**), δ 9.54 (d, J = 5.0 Hz, 1H, **1**), δ 9.50 (d, J = 4.5 Hz, 1H, **1**), δ 9.42 (m, 5H, **1**), δ 9.36 (m, 2H, **1**), δ 9.31 (m, 2H, **1**), δ 9.29 (d, J = 5.7 Hz, 1H, **1**), δ 9.25 (m, 4H, **1**), δ 9.21 (d, J = 5.0 Hz, 1H, **1**), δ 9.15 (m, 3H, **1**), δ 9.04 (d, J = 5.0 Hz, 1H, **1**), δ 9.01 (d, J = 5.7 Hz, 1H, **1**), δ 8.99 (d, J = 5.0 Hz, 1H, **1**), δ 8.84 (m, 4H, **1**), δ 8.79 (d, J = 5.7 Hz, 1H, **1**), δ 8.76 (d, J = 5.7 Hz, 1H, **1**), δ 8.72 (m, 3H, **1**), δ 8.64 (m, 3H, **1**), δ 8.52 (d, J = 4.4 Hz, 1H, **1**), δ 8.49 (d, J = 4.4 Hz, 1H, **1**), δ 8.45 (d, J = 4.4 Hz, 1H, **1**), δ 8.35 (d, J = 4.4 Hz, 1H, **1**), δ 8.22 (d, J = 4.4 Hz, 1H, **1**), δ 8.12 (d, J = 4.4 Hz, 1H, **1**), δ 5.99 (s, 1H, **2**), δ 5.88 (t, J = 6.9 Hz, 1H, **2**), δ 5.70 (d, J = 7.5 Hz, 1H, **2**), δ 5.43 (t, J = 6.9 Hz, 1H, **2**), δ 5.37 (t, J = 6.9 Hz, 1H, **2**), δ 4.85 (d, J = 7.5 Hz, 1H, **2**), δ 4.63 (d, J = 7.0 Hz, 1H, **2**), δ 4.35 (t, J = 6.9 Hz, 1H, **2**), δ 3.99 (t, J = 8.8 Hz, 1H, **2**), δ 3.67 (d, J = 7.0 Hz, 1H, **2**), δ 3.17 (m, 24H, **1**), δ 2.73 (m, 72H, **1**), δ 2.54 (s, 3H, **2**), δ 2.45 (s, 1H, **2**), δ 1.29 (d, J = 6.0 Hz, 2H, **2**), δ 0.99 (d, J = 8.0 Hz, 1H, **2**), δ -0.86 (t, J = 12.8 Hz, 1H, **2**), δ -1.89 (d, J = 5.5 Hz, 3H, **2**). ^{13}C NMR (125 MHz, D_2O, 27 °C, TMS as external standard): δ 174.2 (*C*O, **2**), δ 173.0 (*C*O, **2**), δ 172.6 (*C*O, **2**), δ 169.4–168.0 (*C*q, **1**), δ 166.7 (*C*O, **2**), δ 153.2-151.7 (*C*H, **1**), δ 146.9-144.8 (*C*q, **1**), δ 134.6 (*C*q, **2**), δ 133.9 (*C*q, **2**), δ 126.8-125.8 (*C*H, **1**), δ 124.8 (*C*q, **2**), δ 124.6 (*C*H, **2**), δ 123.9 (*C*q, **2**), δ 122.1 (*C*H, **2**), δ 121.5 (*C*H, **2**), δ 120.9 (*C*H, **2**), δ 119.7 (*C*H, **2**), δ 118.9 (*C*H, **2**), δ 117.8 (*C*H, **2**), δ 116.6 (*C*H, **2**), δ 109.9 (*C*H, **2**), δ 109.1 (*C*H, **2**), δ 108.6 (*C*q, **2**), δ 107.6 (*C*q, **2**), δ 62.9 (CH_2, **1**), δ 56.2 (*C*H, **2**), δ 50.5 (CH_3, **1**), δ 47.2 (*C*H, **2**), δ 28.7 (CH_2, **2**), δ 27.1 (CH_2, **2**), δ 22.2 (CH_3, **2**), δ 13.9 (CH_3, **2**). IR (KBr, cm^{-1}): 3412 (br), 3098, 3017, 2988, 2923, 1664, 1655, 1573, 1522, 1381, 1060, 810. Mp.: 212-228 °C (dec.). Elemental analysis calcd. for $C_{135}H_{174}N_{54}O_{40}Pd_6 \cdot 34H_2O$: C, 36.48; H, 5.49; N, 17.02. Found: C, 36.36; H, 5.14; N, 16.73.

Crystal data of 1•2

$C_{135}H_{202}N_{54}O_{54}Pd_6$, M = 4083.90, Monoclinic, space group C 2/c, cell parameters a = 70.38(1), b = 17.181(3), c = 42.159(8) Å, β = 99.90(3)°, V = 50217(2) Å^3, T = 15(2) K, Z = 8, D_c = 1.068 g cm^{-3}, λ (synchrotron) = 0.6890 Å, 142086 reflections measured, 47250 unique (R_{int} = 0.0714) which were used in all calculations. The structure was solved by direct method (SHELXL-97) and refined by full-matrix least-squares methods on F^2 with 2114 parameters. R_1 = 0.1518 ($I > 2\sigma(I)$) and wR_2 = 0.4521, GOF = 1.378; max./min. residual density 1.532/-1.824 eÅ^{-3}. CCDC reference number 247331. It is noteworthy that in the crystal of **1•2**, the 12 nitrate anions as well as the water molecules were highly disordered, giving rise to a large R_1 value. However, the guest molecule was found from Fourier difference maps and only minor disorder over the peptide backbone chain was found.

2.5 References

1 (a) S. M. Albelda, C. A. Buck, *FASEB J.* **1990**, *4*, 2868. (b) S. Jones, J. M. Thornton, *Proc. Natl. Acad. Sci. U.S.A.* **1996**, *93*, 13. (c) W. E. Stites, *Chem. Rev.* **1997**, *97*, 1233.

2 M. W. Peczuh, A. D. Hamilton, *Chem. Rev.* **2000**, *100*, 2479.

3 (a) S. S. Yoon, W. C. Still, *J. Am. Chem. Soc.* **1993**, *115*, 823. (b) S. R. LaBrenz, J. W. Kelly, *J. Am. Chem. Soc.* **1995**, *117*, 1655. (c) C.-T. Chen, H. Wagner, W. C. Still, *Science* **1998**, *279*, 851. (d) M. A. Hossain, H.-J. Schneider, *J. Am. Chem. Soc.* **1998**, *120*, 11208. (e) K. B. Jensen, T. M. Braxmeier, M. Demarcus, J. G. Frey, J. D. Kilburn, *Chem. Eur. J.* **2002**, *8*, 1300. (f) K. Tsubaki, T. Kusumoto, N. Hayashi, M. Nuruzzarman, K. Fuji, *Org. Lett.* **2002**, *4*, 2313. (g) C. Schmuck, L. Geiger, *J. Am. Chem. Soc.* **2004**, *126*, 8898. (h) R. Zadmard, M. Arendt, T. Schrader, *J. Am. Chem. Soc.* **2004**, *126*, 7752. (i) A. Ojida, Y. Miyahara, T. Kohira, I. Hamachi, *Biopolymers*, **2004**, *76*, 177. (j) M. Kruppa, C. Mandl, S. Miltschitzky, B. König, *J. Am. Chem. Soc.* **2005**, *127*, 3362. (k) M. Fokkens, T. Schrader, F.-G. Klärner, *J. Am. Chem. Soc.* **2005**, *127*, 14415.

4 (a) J. S. Albert, M. S. Goodman, A. D. Hamilton, *J. Am. Chem. Soc.* **1995**, *117*, 1143. (b) M. W. Peczuh, A. D. Hamilton, J. Sánchez-Quesada, J. Mendoza, T. Haack, E. Giralt, *J. Am. Chem. Soc.* **1997**, *119*, 9327. (c) Y. Hamuro, M. C. Calama, H. S. Park, A. D. Hamilton, *Angew. Chem., Int. Ed. Engl.* **1997**, *36*, 2680. (d) H. S. Park, Q. Lin, A. D. Hamilton, *J. Am. Chem. Soc.* **1999**, *121*, 8.

5 A. A. Bogan, K. S. Thorn, *J. Mol. Biol.* **1998**, *280*, 1.

6 (a) E. A. Padlan, *Mol. Immunol.* **1994**, *31*, 169. (b) K. Tsumoto, K. Ogasahara, Y. Ueda, K.

Watanabe, K Yutani, I. Kumagai, *J. Biol. Chem.* **1995**, *270*, 18551.

7 (a) R. Ueoka, Y. Matsumoto, K. Harada, H. Akahoshi, Y. Ihara, Y. Kato, *J. Am. Chem. Soc.* **1992**, *114*, 8339. (b) M. Maletic, H. Wennemers, D. Q. McDnald, R. Breslow, W. C. Still, *Angew. Chem., Int. Ed. Engl.* **1996**, *35*, 1490. (c) R. Breslow, Z. Yang, R. Ching, G. Trojandt, F. Odobel, *J. Am .Chem. Soc.* **1998**, *120*, 3536. (d) D. Wilson, L. Perlson, R. Breslow, *Bioorg. Med. Chem.* **2003**, *11*, 2649.

8 (a) M. Fujita, D. Oguro, M. Miyazawa, H. Oka, K. Yamaguchi, K. Ogura, *Nature* **1995**, *378*, 469. (b) T. Kusukawa, M. Fujita, *J. Am. Chem. Soc.* **2002**, *124*, 13576. (c) M. Yoshizawa, M. Tamura, M. Fujita, *J. Am. Chem. Soc.* **2004**, *126*, 6846. (d) M. Yoshizawa, S. Miyagi, M. Kawano, K. Ishiguro, M. Fujita, *J. Am. Chem. Soc.* **2004**, *126*, 9172.

9 Association constants were measured by the UV titration at a charge transfer band in water. Spectra were analyzed by a nonlinear curve-fitting procedure.

10 Since UV titrations of **1•2** showed the saturation at nearly 1 equiv of **1**, exact value of K_a could not be calculated by this measurement. Thus, K_a was estimated to be 10^6 M^{-1}.

11 Four triazine ligands composing cage **1** are highly electron deficient due to multiple electron withdrawing from three palladium cations.

12 (a) M. Fujita, K. Umemoto, M. Yoshizawa, N. Fujita, T. Kusukawa, K. Biradha, *Chem. Commun.* **2001**, 509. (b) K. Kumazawa, K. Biradha, T. Kusukawa, T. Okano, M. Fujita, *Angew. Chem. Int. Ed.* **2003**, *42*, 3909. (c) J.-P. Bourgeois, M. Fujita, M. Kawano, S. Sakamoto, K. Yamaguchi, *J. Am. Chem. Soc.* **2003**, *125*, 9260.

13 F. Ibukuro, T. Kusukawa, M. Fujita, *J. Am. Chem. Soc.* **1998**, *120*, 8561.

Chapter 3

A Porphyrin Capsule as a Smart Peptide Receptor : Specific Binding of Aromatic Peptides and Modulation of Selectivity via Changing of Porphyrin Metal Ions

Abstract

The porphyrin prism complex showed not only high selectivity, but also very high affinity with a Tyr-Tyr sequence in water (K_a = $10^{8\text{-}9}$ M^{-1}). This value was comparable with that of biological recognition system such as antibody-antigen interaction. On the other hand, sequence-selectivity could be controlled by changing the porphyrin metal ions from Zn^{2+} to Au^{3+}.

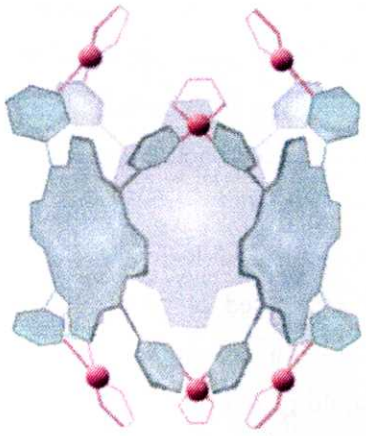

Zn(II)-porphyrin prism

High affinity & High selectivity in Water

Tyr-Tyr-Ala $K_a = 10^8\ M^{-1}$

Tyr-Ala-Tyr $K_a = 10^3\ M^{-1}$

3.1 Introduction

The peptide is considered extremely important targets in the chemistry of molecular recognition due to its difficulty and utility. The selectivity is one of difficulty of peptide recognition. Because the peptides possessing various functional groups have complicate and relatively large structure more than general organic molecules used in host-guest chemistry, therefore we have to design and synthesize elaborate receptors for peptide recognition.[1] Another difficulty and importance in peptide recognition is strong binding in water. Generally, designed peptide receptors exhibit slight affinity in water, because many artificial receptors interact with peptides through mainly hydrogen bonding. Recently, a few sophisticated receptors made it come true moderate binding of peptides even in water (K_a = $10^{4\sim5}$ M^{-1}).[2] The key points of moderate binding are multi-point interaction and hydrophobic effect that enhanced in water.

Ultimate example of strong recognition is proteins as receptor. Some proteins such as antibody and enzyme can bind substrates very strongly (K_a = $10^{6\sim10}$ M^{-1}).[3] The essence of strong recognition by proteins is seem to be large and hydrophobic binding pocket on protein surface. This pocket allows efficient hydrophobic interaction and a large number of multi-point interactions between substrates and various side chains of amino acids on protein surface.

Cyclodextrin is one of superior and available receptors in terms of molecular recognition in water due to its hydrophobic cavity. Indeed, some cyclodextrin derivatives have been used in amino acids and peptide recognition.[4] However, the cavity is relatively small, thus cyclodextrin dimers, connected by organic linkers, were synthesized for the peptide recognition.[5] For this reason, using the cyclodextrin derivatives is seem to be limit in peptide recognition. Thus, the design of novel artificial receptors possessing large hydrophobic pocket enough to bind oligopeptides is absolutely essential.

We have demonstrated the recognition of large organic substrates up to four molecules by self-assembled coordination cages.[6] These receptors are composed of panel-like organic ligands and cis-protected palladium(II) ions, and have large hydrophobic cavities.[7] In chapter 2, we found that the cavity of a coordination cage could recognize tripeptide, Ac-Trp-Trp-Ala-NH_2, strongly (K_a = 10^6 M^{-1}) with sequence-selective fashion. If we can design an ideal peptide receptor that interacts more tightly by perfectly hydrophobic wrapping of peptides, we expect to achieve stronger binding of peptide in water comparable with biological system such as antibody-antigen. Here, we exhibit more excellent peptide recognitions by self-assembled porphyrin capsules,[8] namely this receptor bound peptides very strongly (K_a = $10^{8\sim9}$ M^{-1}) and very selectively.

3.2 Result and Discussion

3.2.1 Synthesis and self-assembly of Zn(II)-porphyrin capsule **1**

Self-assembly of Zn-porphyrin capsule **1** was already reported in early paper.[8] Zinc 5,10,15,20-tetra(3-pyridyl)-12*H*,23*H*-porphine and *cis*-protected Pd(II) complex were self-assembled into Zn(II)-porphyrin capsule **1** quantitatively in water.

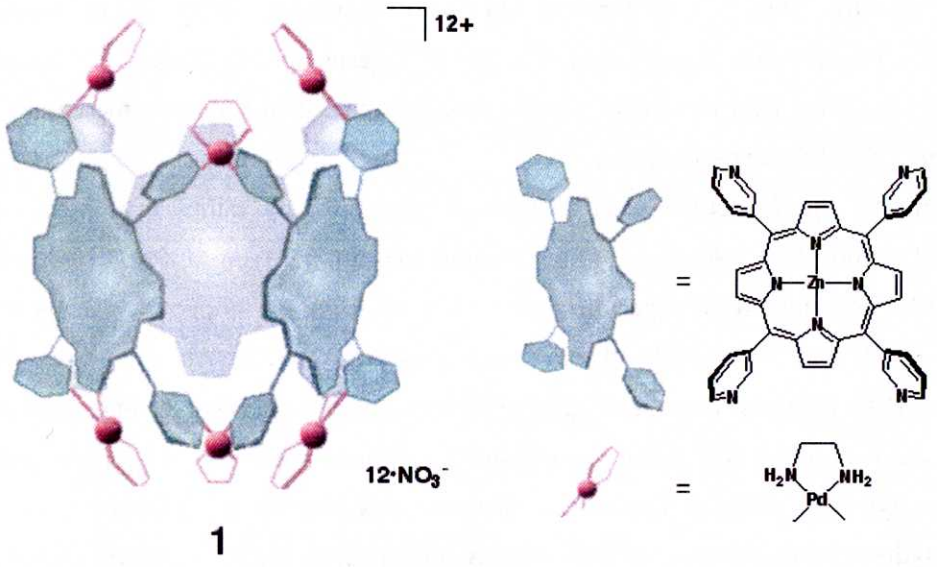

3.2.2 Strong binding of Tyr-Tyr-Ala sequence by Zn(II)-porphyrin capsule **1**

In previous chapter, coordination cage showed high affinity with Trp-Trp-Ala sequence in water ($K_a > 10^6$ M^{-1}). However, in the case of Zn(II)-porphyrin capsule **1**, this selectivity dramatically changed. In fact, the capsule **1** selectively bound Ac-Tyr-Tyr-Ala-NH_2 (**2**) rather than Ac-Trp-Trp-Ala-NH_2 (**3**). When the same amount of peptide **2** and **3** were added to the aqueous solution of **1**, only complex **1•2** was formed.

To estimate the difference of affinity quantitatively, binding constants of peptides and Zn-porphyrin capsule **1** were evaluated. The K_a of **1•3** was measured by the UV-vis titration in water and spectra were analyzed by a nonlinear curve-fitting procedure. As a result, K_a of **1•3** were determined to be 4 x 10^5 M^{-1}. On the other hand, since UV-vis titration of **1•2** was saturated at nearly 1 equiv of **2**, exact value of K_a could not be calculated by this measurement. For determination of the accurate value of K_a of complex **1•2**, we carried out ^{1}H NMR competition experiments referenced to absolute binding constants measured by UV-vis titration. At first, K_a of complex **1** and Ac-Ala-Ala-Ala-NH_2 (**4**) was calculated to be 1 x 10^6

M^{-1} by ^1H NMR competition experiment with equimolar amount of **3**. Furthermore, we measured K_a of **1•2** by ^1H NMR competition with equemolar amount of **4**. Interestingly, we found that binding constant of **1•2** showed 2 x 10^8 M^{-1} even in water, whose value is comparable with antibody–biomolecules interactions in nature.

3.2.3 Sequence-selective recognition of Tyr-rich Tripeptide by Zn-porphyrin capsule **1**

In addition to strong association of complex **1•2**, we observed strict sequence-selectivity among the similar sequences, Ac-Tyr-Tyr-Ala-NH_2 (**3**), Ac-Tyr-Ala-Tyr-NH_2 (**5**) and Ac-Ala-Tyr-Tyr-NH_2 (**6**). The K_a's of **1•5** and **1•6** could be determined by UV-vis titration and competition experiment (2 x 10^3 and 4 x 10^5 M^{-1}, respectively) (Table 1). Namely, the peptide **2** was bound by **1** more than 100000-times stronger than **5**, despite these peptides had same residues in different sequences.

Furthermore, the **1** recognized Tyr residues most strongly rather than other aromatic residues, Trp and Phe. We estimated the binding constant between Ac-Phe-Phe-Ala-NH_2 (**7**) and **1** by NMR competition experiment (K_a = 4 x 10^7 M^{-1}). The peptide **7** showed strong affinity with **1**, thus we considered that phenyl rings in Xxx-Xxx-Ala sequence, where the Xxx is aromatic residues, were most suitable with cavity of **1**, and indole rings were so bulky that peptide **3** showed lower affinity than **2** and **7**. From comparison of K_a values between **2** and **7**, the hydroxyl group at Tyr residues seemed to be important. Therefore, we suppose that the hydroxyl group of Tyr residues slightly interact with Zn(II) porphyrin metals at each ligands.

In addition to the sequence selectivity in aromatic peptides, porphyrin capsule **1** showed high selectivity in aliphatic peptides. In several Ac-Xxx-Xxx-Xxx-NH_2 peptides, where the Xxx is aliphatic residues, only Ala-Ala-Ala sequence was recognized strongly. On the other hand, other aliphatic peptides, Ac-Gly-Gly-Gly-NH_2 (**8**), Ac-Val-Val-Val-NH_2 (**9**) and Ac-Leu-Leu-Leu-NH_2 (**10**) were not bound in **1**. This selectivity is discussed in Chapter 6.

3.2.4 Discussion about solution structure of complex **1•2**

To estimate the geometry of **2** within the Zn-porphyrin capsule **1**, ^1H NMR of complex **1•2** was measured and each signals of **2** were assigned from TOCSY and NOESY experiments (Figure 1). NMR signals of Tyr1 and Tyr2 residues were highly up-field shifted. In particular, Hα of Tyr1 signal was observed at –5.5 ppm, that is up-field shifted more than 10 ppm compared with free peptide. This result indicates that Tyr residues are close to porphyrin ligands, namely Tyr residues are encapsulated in capsule. On the other hand, each signals of Ala3 showed little up-field shift, suggesting that Ala locate at outside of the capsule

1.

Interestingly, signals of **1** in aromatic region were observed in a very complex pattern indicating the desymmetrization of the prism **1**. The motion of **2** is highly restricted by enclathration, and therefore all porphyrin protons of **1** become inequivalent.

Table 1. Association constants of **1** with tripeptides in water at 27 °C

Peptides	K_a (M^{-1})
Ac-***Tyr-Tyr-***Ala-NH_2 (**2**)[a]	2 x 10^8
Ac-***Tyr-***Ala-***Tyr-***NH_2 (**5**)[b]	2 x 10^3
Ac-Ala-***Tyr-Tyr-***NH_2 (**6**)[a]	4 x 10^5
Ac-Trp-Trp-Ala-NH_2 (**3**)[b]	4 x 10^5
Ac-Phe-Phe-Ala-NH_2 (**7**)[a]	4 x 10^7
Ac-Ala-Ala-Ala-NH_2 (**4**)[c]	1 x 10^6
Ac-Gly-Gly-Gly-NH_2 (**8**)	no binding
Ac-Val-Val-Val-NH_2 (**9**)	no binding
Ac-Leu-Leu-Leu-NH_2 (**10**)	no binding

[a] Measured by NMR competition experiment with **4**. [b] Measured by UV-titration. [c] Measured by NMR competition experiment with **3**.

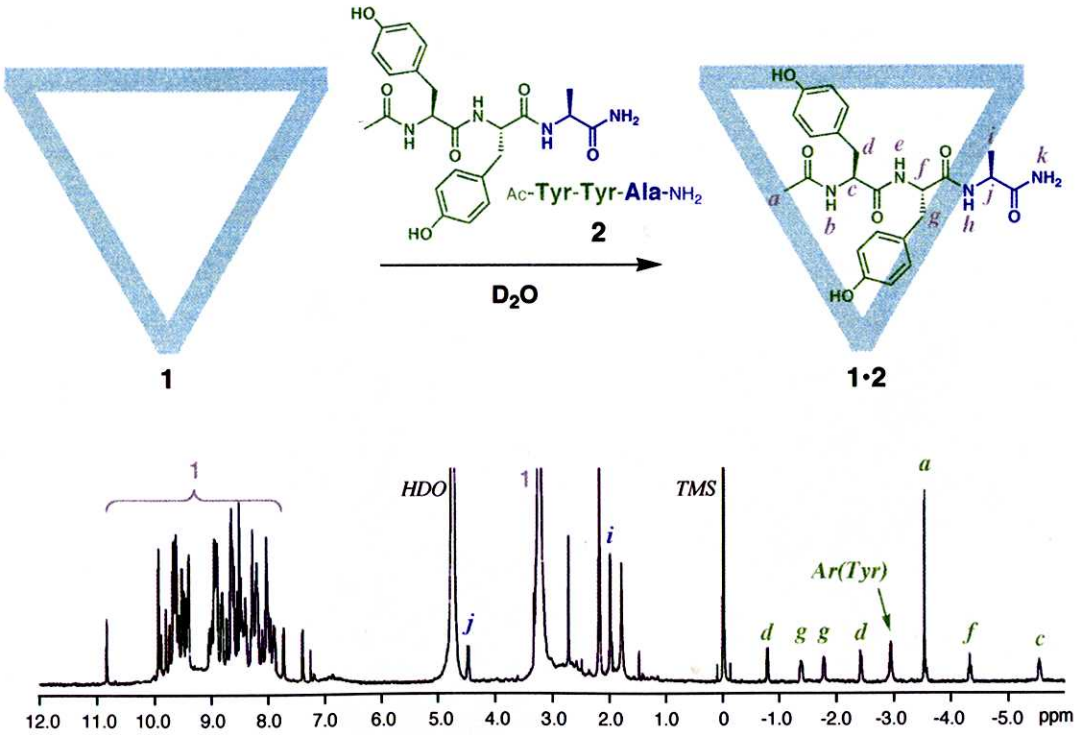

Figure 1. ^{1}H NMR spectrum of complex **1•2** (500 MHz, D_2O, 300 K, 2 mM) and schematic representation of complex formation.

The conformation of **2** in the capsule **1** was also studied by molecular dynamics (MD) simulation with CNS program[9] that run under NOE distance restraints (5 intra-residue, 3 sequential, 2 medium-range). Figure 2 exhibited the superimposition of the 15 lowest-energy structures for **2**. Although two aromatic rings and C-terminal were highly disordered due to difficulty of NOE observation in these protons, backbone conformation of **2** could be almost determined by CNS calculation. Furthermore, we confirmed the MD minimized structure fits the cavity of **1**. Figure 3 showed the refined structure of the combined complex **1•2**, suggesting that peptide **2** was tightly accommodated in **1**. This result agreed with the NMR observation indicating that the motion of **2** was highly restricted in **1**.

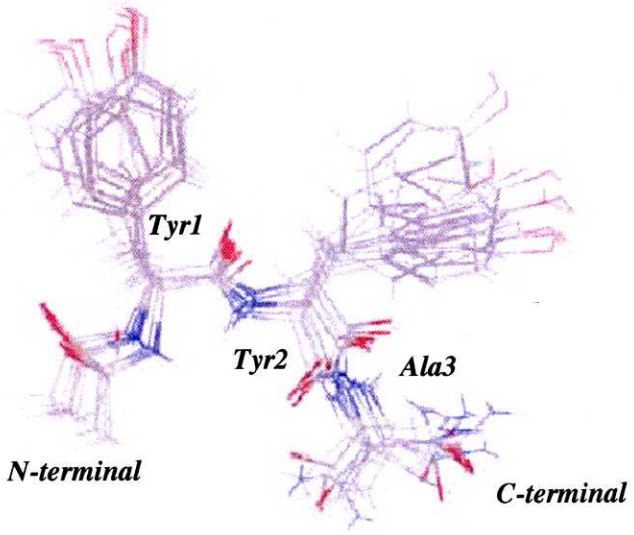

Figure 2. Superposition of the 12 lowest energy structures by CNS[9] for bound peptide **2**.

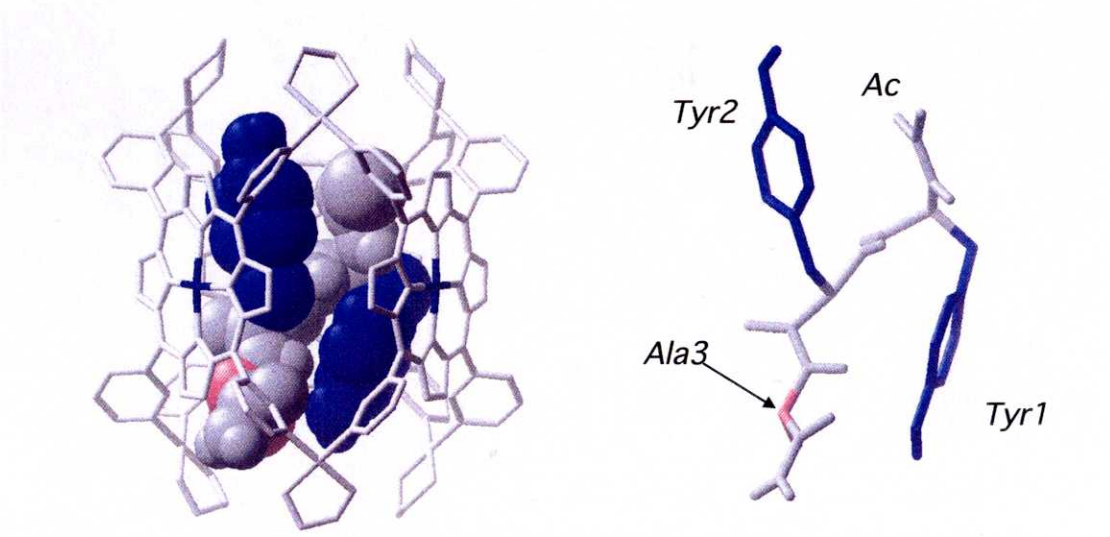

Figure 3. Refined structure of complex **1•2** from **1** and MD minimized structure of **2**.

3.2.5 Determination of the ideal peptide sequence for the cavity of **1**

From ^{1}H NMR of complex **1•2**, the Ala3 seemed to locate at outside of capsule. Thus, we expected that Ac-Tyr-Tyr-NH_2 (**11**), removed Ala residue from **2**, show higher association constant than **2**. In fact, peptide **11** was bound very strongly in **1** (K_a = 4 x 10^9 M^{-1}). This value was calculated from competition experiment of ^{1}H NMR between **1** (5 μmol) and **11** (1 μmol). Therefore, we concluded that Tyr-Tyr sequence is ideal for the cavity of **1**.

3.2.6 Site-selective recognition of polypeptide chain by **1**

In tripeptide recognition, the **1** recognized Tyr-Tyr sequence with high affinity. This selectivity is applicable to the site-selective recognition of longer polypeptide chain. We designed 9-residue peptide, Ac-Tyr-Tyr-Ala-Gly-Phe-Asn-Thr-Ser-Gly-NH_2 (**12**), possessing Tyr-Tyr sequence at N-terminal. In fact, capsule **1** could bound only N-terminal Tyr-Tyr sequence, despite the **12** had one aromatic Phe residue at middle. The **1•12** complex was prepared by mixing of both aqueous solution (2 mM) at room temperature for several minutes. In ^{1}H NMR, only Tyr-Tyr region was highly up-field shifted such as complex **1•2**.

3.2.7 Zn(II)-porphyrin capsule **1** vs. Au(III)-porphyrin capsule **13**

Generally, Au(III)-porphyrin possesses electron acceptor property compared with Zn(II)-porphyrin possessing electron donor property. Additionally, Au(III)-porphyrin is cationic (+1). Therefore, the sequence-selectivity of Au(III)-porphyrin capsule **13** is expected to change compared with Zn(II)-porphyrin capsule **1**. We expected that the cavity of capsule **13** is more hydrophilic than **1** and provides more electron deficient environment.

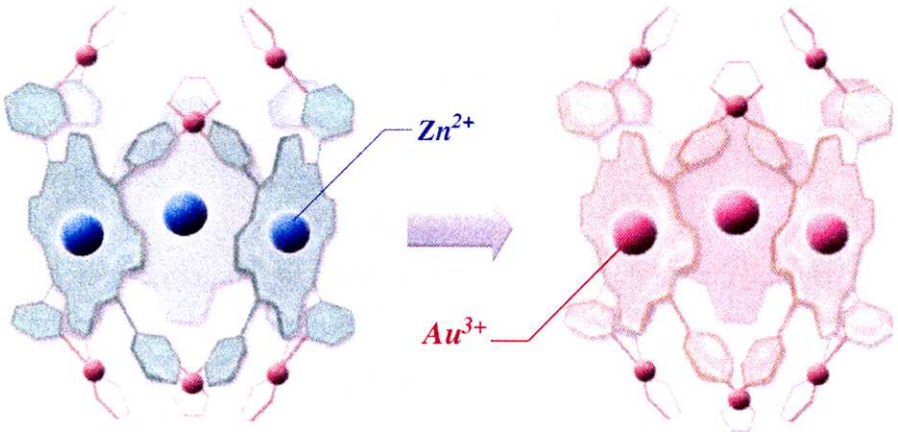

Two porphyrin capsule **1** and **13** could be easily prepared by similar procedure. In a similar way, the Au-porphyrin capsule **13** was synthesized, namely gold 5,10,15,20-tetra(3-pyridyl)-12*H*,23*H*-porphine and *cis*-protected Pd(II) complex were self-assembled into Au-porphyrin capsule **13**. From ^{1}H NMR, solution structure of **13** was similar to **1**.

The K_a of several peptides and Au-capsule **13** were measured from UV-vis titrations (Table 2). Indeed, Ac-Trp-Trp-Ala-HN_2 (**3**) was recognized stronger than Ac-Tyr-Tyr-Ala-NH_2 (**2**) by Au(III)-capsule **13**. These result indicate that electron-deficient Au(III)-capsule **13** bound efficiently electron-rich residue, namely Trp than Tyr, due probably to charge transfer interaction between Au(III)-porphyrin and aromatic rings of bound peptide.

Table 2. Association constants of **13** with tripeptides in water

Peptides	K_a (M^{-1})[a]
Ac-Tyr-Tyr-Ala-NH_2 (**2**)	6×10^4
Ac-Trp-Trp-Ala-NH_2 (**3**)	9×10^5

[a] Measured by UV-vis titration at 20 °C.

3.3 Conclusion

In conclusion, we carried out quite strong and selective peptide recognition by using the porphyrin capsule **1**. The Zn-porphyrin capsule **1** recognized Tyr-Tyr-Ala sequence very strongly ($K_a = 2 \times 10^8$ M^{-1}). Since the NMR studies indicated that Ala residue of Tyr-Tyr-Ala was located at outside of **1**, we could design the ideal sequence, Tyr-Tyr, for the Zn-capsule **1**. Furthermore, **1** could perfectly discriminate the very similar sequences, Tyr-Tyr-Ala, Tyr-Ala-Tyr and Ala-Tyr-Tyr, and various selectivity was observed in aromatic and aliphatic peptide recognition. These selectivity was also applied to the site-selective recognition of longer polypeptide chain. On the other hand, Au-capsule **13** preferred to Trp-Trp-Ala sequence rather than Tyr-Tyr-Ala sequence. Namely, we could control the sequence-sequence selectivity by changing the prophyrin metal ion. This result suggests that porphyrin capsule is superb scaffold for the peptide recognition, because we can do fine-tuning the sequence-selectivity by changing the porphyrin metal ion from Zn(II) to various metal ions.

3.4 Experimental Section

Peptide synthesis, procedure of UV titration, NMR measurements, competition experiment and structural calculations by CNS were described in General Experimental Section. The porphyrin cage **1** was prepared following procedure as reported earlier.[8]

Physical data of 1•2

^{1}H NMR (500 MHz, D_2O, 27 °C, TMS as external standard): δ 10.83 (s, 1H, **1**), δ 9.93 (s, 2H, **1**), δ 9.88 (d, J = 6.0 Hz, 1H, **1**), δ 9.80 (s, 1H, **1**), δ 9.73 (d, J = 5.1 Hz, 1H, **1**), δ 9.68-9.64 (m, 5H, **1**), δ 9.63-9.58 (m, 5H, **1**), δ 9.57 (d, 1H, **1**), δ 9.52 (s, 2H, **1**), δ 9.51 (s, 1H, **1**), δ 9.49 (s, 1H, **1**), δ 9.45 (s, 1H, **1**), δ 9.42 (s, 1H,**1**), δ 9.39 (d, J = 7.7 Hz, 2H, **1**), δ 9.03 (d, J = 7.7 Hz, 1H, **1**), δ 8.99 (d, J = 7.7 Hz, 1H, **1**), δ 8.96 (s, 1H, **1**), δ 8.95 (s, 2H, **1**), δ 8.94-8.93 (m, 5H, **1**), δ 8.92-8.89 (m, 5H, **1**), δ 8.88 (s, 1H, **1**), δ 8.84-8.80 (m, 5H, **1**), δ 8.73 (s, 1H, **1**), δ 8.72 (s, 1H, **1**), δ 8.67 (s, 1H, **1**), δ 8.66 (s, 1H, **1**), δ 8.65 (s, 1H, **1**), δ 8.64 (br, 1H, **1**), δ 8.63 (br, 1H, **1**), δ 8.61 (br, 2H, **1**), δ 8.60 (br, 2H, **1**), δ 8.59 (s, 1H, **1**), δ 8.55 (m, 5H, **1**), δ 8.51 (br, 8H, **1**), δ 8.49 (br, 1H, **1**), δ 8.48 (br, 2H, **1**), δ 8.45 (d, J = 6.8 Hz, 1H, **1**), δ 8.42 (d, J = 6.8 Hz, 1H, **1**), δ 8.40 (s, 2H, **1**), δ 8.38 (s, 1H, **1**), δ 8.31 (s, 1H, **1**), δ 8.29 (s, 1H, **1**), δ 8.28 (s, 1H, **1**), δ 8.27 (s, 1H, **1**), δ 8.26 (s, 1H, **1**), δ 8.24 (s, 1H, **1**), δ 8.23 (s, 1H, **1**), δ 8.22-8.16 (m, 12H, **1**), δ 8.10 (t, J = 6.0 Hz, 2H, **1**), δ 8.05-7.99 (m, 12H, **1**), δ 7.98 (s, 1H, **1**), δ 7.95 (d, J = 4.3 Hz, 1H, **1**), δ 7.92 (s, 1H, **1**), δ 7.91-7.88 (m, 4H, **1**), δ 7.87 (s, 1H, **1**), δ 7.73 (d, J = 4.3 Hz, 1H, **1**), δ 7.39 (d, J = 4.3 Hz, 1H, **1**), δ 4.47 (q, J = 6.8 Hz, 1H, **2**), δ 3.33-3.10 (m, 24H, **1**), δ 2.00 (d, J = 6.8 Hz, 3H, **2**), δ -0.78 (d, J = 8.5 Hz, 1H, **2**), δ -1.37 (dd, J = 7.7, 6.0 Hz, 1H, **2**), δ -1.77 (dd, J = 6.0, 6.0 Hz, 1H, **2**), δ -2.41 (d, J = 13.7 Hz, 1H, **2**), δ -2.93 (br, 2H, **2**), δ -3.52 (s, 3H, **2**), δ -4.30 (t, J = 12.8 Hz, 1H, **2**), δ -5.53 (dd, J = 8.5, 5.1 Hz, 1H, **2**).

^{13}C NMR (125 MHz, D_2O, 27 °C, TMS as external standard): δ 177.3 (CO, **2**), δ 173.9 (CO, **2**), δ 171.1 (CO, **2**), δ 167.5 (CO, **2**), δ 155.0–152.5 (CH, **1**), δ 152.3–148.3 (CH, **1**), δ 147.6–145.2 (CH, **1**), δ 142.4–140.8 (Cq, **1**), δ 133.7–130.2 (CH, **1**), δ 126.3–124.5 (CH, **1**), δ 123.1 (CH, **2**), δ 121.7 (CH, **2**), δ 115.6–113.5 (Cq, **1**), δ 47.1 (CH_2, **1**), δ 49.3 (CH, **2**), δ 48.2 (CH, **2**), δ 48.5 (CH, **2**), δ 32.1 (CH, **2**), δ 32.0 (CH, **2**), δ 25.9 (CH, **2**), δ 19.0 (CH, **2**), δ 17.1 (CH_3, **2**).

IR (KBr, cm^{-1}): 1563.3, 1515.4, 1475.5, 1383.9, 1243.5, 1192.7, 1111.0, 1056.5, 1036.2, 994.8, 796.6, 698.6.

Synthesis of Hexafluorophosphate[5,10,15,20-tetra(3-pyridyl)porphyrinato]aurate(III)

The 5,10,15,20-tetra(3-pyridyl)-21H,23Hporphyrin (1.644 g, 2.66 mmol) together with $KAuCl_4$ (2.045 g, 5.32 mmol) and sodium acetate (1.091 g, 13.3 mmol) were dissolved in glacial acetic acid (25 cm^3). The resulting purple solution was purged with argon and then heated at reflux temperature under inert atmosphere for 8 h, the flask being wrapped in aluminium foil to shield from the light. After reaction, glacial acetic acid was removed under reduced pressure and the residue taken up into dichloromethane. The solution was washed with saturated aqueous solution of $NaHCO_3$ followed by a saturated aqueous solution of KPF_6 and finally water. After drying over anhydrous sodium sulfate, the solvent was removed and the crude product purified by column chromatography on silica gel (dichloromethane : methanol = 10 : 1) (0.797 g, 37%).

^1H NMR (500 MHz, $CDCl_3$, 50 °C, TMS as internal standard): δ=9.49 (br, 4H), 9.27 (s, 8H), 9.17 (d, *J*=5 Hz, 4H), 8.61 (br, 4H), 7.85 (dd, *J*= 5 Hz, >1 Hz, 4H) (ppm).

^{13}C NMR (125 MHz, $CDCl_3$, TMS as internal standard) δ =152.549 (CH), 150.920 (CH), 141.288 (CH), 137.208 (Cq), 134.648 (Cq), 132.433 (CH), 123.153 (CH), 120.248 (Cq) (ppm).

^{31}P NMR(202.5 MHz, $CDCl_3$, 85% phosphoric acid as external standard) δ= −146.68 (hept, *J* = 714.6 Hz, PF_6).

IR (KBr) 1587.0, 1566.5, 1475.5, 1410.0, 1362.8, 1320.9, 1190.2, 1086.7, 1062.4, 1039.4, 1021.4, 840.4, 798.8, 716.7 (cm-1).

UV-vis ($CHCl_3$) λ_{max} (ε) [nm (cm^{-1} M^{-1})] 300 (11980); 407 (156790); 522 (15990).

Synthesis and physical data of 13

Hexafluorophosphate[5,10,15,20-tetra(3-pyridyl)porphyrinato]aurate(III) (344.5 mg, 1.62 mmol) was reacted with *cis*-ethylenediaminedinitrato palladium(II) (0.939 g, 3.23 mmol) in water-acetonitrile 1:1 mixed solvent at 80 °C for 1 day. Acetone (150 mL) was added to the dark red reaction solution then precipitate was separated by centrifuge. The dark red powder was dried in vacuo then gave the porphyrin prism complex [**13**•$(NO_3^-)_{12}$•$(PF_6^-)_3$].

^1H NMR (500 MHz, CD_3CN : D_2O = 1 : 1, TMS as external standard): δ 10.11 (d, *J* = 5.5 Hz, 12H), δ 9.99 (s, 12H), δ 9.50 (s, 12H), δ 9.42 (s, 12H) δ 9.00 (d, *J* = 8.0 Hz, 12H), δ 8.57 (dd, *J* = 1.5, 6.0 Hz, 12H), δ 3.55~3.49, δ 3.48~3.42 (m, 24H) (ppm).

^{13}C NMR (125 MHz, CD_3CN : D_2O = 1 : 1, TMS as external standard) δ 153.980 (CH), δ 150.296 (CH), δ 146.122 (CH), δ 137.957 (Cq), δ 137.641 (Cq), δ 137.541 (Cq), δ 133.058 (CH), δ 132.563 (CH), δ 126.799 (CH), δ 118.185 (CH), δ 47.574 (CH_2) (ppm).

^{31}P NMR (202.5 MHz, CD_3CN : D_2O = 1 : 1, 85% phosphoric acid as external standard) δ=

−144.99 (hept, J = 708.6 Hz, PF_6).

IR (KBr) 1478.4, 1384.6, 1194.6, 1134.3, 1054.9, 1037.8, 840.5, 802.9 (cm^{-1}).

UV-vis (H_2O) λ_{max} (ε) [nm (cm^{-1} M^{-1})] 293 (34390), 404 (476440), 485 (7780), 525 (29640).

3.5 References

1 (a) S. S. Yoon, W. C. Still, *J. Am. Chem. Soc.* **1993**, *115*, 823. (b) S. R. LaBrenz, J. W. Kelly, *J. Am. Chem. Soc.* **1995**, *117*, 1655. (c) C.-T. Chen, H. Wagner, W. C. Still, *Science* **1998**, *279*, 851. (d) K. B. Jensen, T. M. Braxmeier, M. Demarcus, J. G. Frey, J. D. Kilburn, *Chem. Eur. J.* **2002**, *8*, 1300. (e) K. Tsubaki, T. Kusumoto, N. Hayashi, M. Nuruzzarman, K. Fuji, *Org. Lett.* **2002**, *4*, 2313.

2 (a) M. A. Hossain, H.-J. Schneider, *J. Am. Chem. Soc.* **1998**, *120*, 11208. (b) C. Schmuck, L. Geiger, *J. Am. Chem. Soc.* **2004**, *126*, 8898. (c) A. Ojida, Y. Miyahara, T. Kohira, I. Hamachi, *Biopolymers*, **2004**, *76*, 177. (d) M. Kruppa, C. Mandl, S. Miltschitzky, B. König, *J. Am. Chem. Soc.* **2005**, *127*, 3362. (e) M. Fokkens, T. Schrader, F.-G. Klärner, *J. Am. Chem. Soc.* **2005**, *127*, 14415.

3 K. N. Houk, A. G. Leach, S. P. Kim, X. Zhang, *Angew. Chem. Int. Ed.* **2003**, *42*, 4872.

4 (a) R. Breslow, B. Zhang, *J. Am. Chem. Soc.* **1992**, *114*, 5882. (b) R. Ueoka, Y. Matsumoto, K. Harada, H. Akahoshi, Y. Ihara, Y. Kato, *J. Am. Chem. Soc.* **1992**, *114*, 8339.

5 (a) Breslow, Z. Yang, R. Ching, G. Trojandt, F. Odobel, *J. Am. Chem. Soc.* **1998**, *120*, 3536. (b) D. Wilson, L. Perlson, R. Breslow, *Bioorg. Med. Chem.* **2003**, *11*, 2649.

6 (a) T. Kusukawa, M. Fujita, *J. Am. Chem. Soc.* **2002**, *124*, 13576. (b) M. Yoshizawa, M. Tamura, M. Fujita, *J. Am. Chem. Soc.* **2004**, *126*, 6846.

7 (a) M. Fujita, *Chem. Soc. Rev.* **1998**, *27*, 417. (b) M. Fujita, K. Umemoto, M. Yoshizawa, N. Fujita, T. Kusukawa, K. Biradha, *Chem. Commun.* **2001**, 509. (c) M. Fujita, M. Tominaga, A. Hori, B. Therrien, *Acc. Chem. Res.* **2005**, *38*, 371.

8 N. Fujita, K. Biradha, M. Fujita, S. Sakamoto, K. Yamaguchi, *Angew. Chem. Int. Ed.* **2001**, *40*, 1718.

9 A. T. Brünger, P. D. Adams, G. M. Clore, W. L. DeLano, P. Gros, R. W. Grosse-kunstleve, J.-S. Jiang, J. Kuszewski, M. Nilges, N. S. Pannu, R. J. Read, L. M. Rice, T. Simonson, G. L. Warren, *Acta Cryst.* **1998**, *D54*, 905–921.

Chapter 4

Folding a Nona-peptide into an α-Helix through Hydrophobic Binding by a Bowl-shaped Host

Abstract

The α-Helical conformation of 9-residue peptide (Trp-Ala-Glu-Ala-Ala-Ala-Glu-Ala-Trp) was induced and stabilized in water by encapsulation within a bowl-shaped coordination host. The bowl-shaped cavity recognized the α-helical peptide through two types of host-guest interactions: primarily, hydrophobic interaction with both terminal Trp residues and, secondarily, electrostatic interaction between the Glu residues and the highly positive charge of host (12+). The ^{1}H NMR revealed that Trp1, Ala5, and Trp9 in *i*, *i*+4, and *i*+8 positions were deeply accommodated in the cavity. The α-helical conformation of peptide was reliably confirmed by NOESY experiments and molecular dynamics simulation.

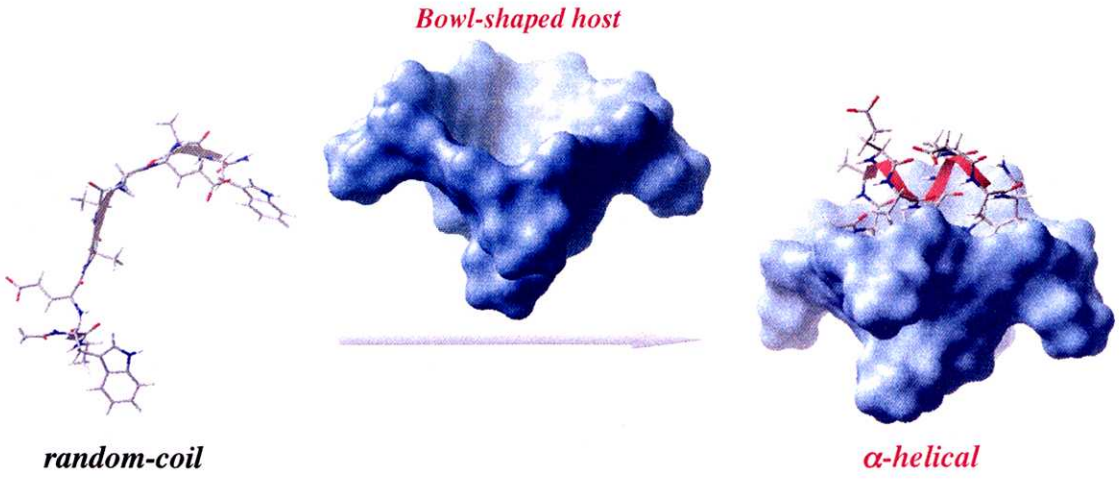

4.1 Introduction

Spontaneous folding of polypeptides into their latent secondary structures like α-helix and β-sheet is both chemically and biologically important processes. It is highly expected that studies on peptide folding leads to the construction of functional architectures with peptide backbone and helps the understanding of protein folding in nature.[1] Extensive studies have been made, therefore, on the formation of peptide secondary structures from de novo designed oligopeptides.[2,3] However, secondary structures from synthetic peptides are normally ephemeral unless fixed by covalent link or metal-coordination among residues.[4-6] In proteins, fragmental units remain stable as they are sustained by protein scaffolds through weak interactions (hydrophobic, electrostatic, etc.). We expect that the large hydrophobic cavity of a synthetic host can replace the protein scaffolds to stabilize the secondary structures of oligopeptides.

4.2 Results and Discussion

4.2.1 Self-assembly of platinum bowl-shaped cavity

To realize the stabilization of α-helical conformation of oligopeptide, several experiments should be carried out in buffer solution. Although phosphate buffer is better one due to its appropriate pH and no hydrocarbons that interrupt some ^{1}H NMR studies, palladium bowl-shaped host, previously synthesized in our laboratory, is unstable in phosphate buffer solution. Therefore, we synthesized platinum bowl-shaped cavity **1** instead of palladium bowl, because Pt-pyridine bond is irreversible at room temperature.

At first, only (en)Pt$(NO_3)_2$ and a triazine-cored tridentate ligand were mixed in water at 90 °C for 1 week. However, some complicated ^{1}H NMR spectra were observed. Therefore, 2-naphtoic acid was added to the aqueous solution of (en)Pt$(NO_3)_2$ and ligand as a template molecule of bow-shaped cavity. As a result, platinum-bowl was self-assembled quantitatively after several days (Scheme 1). After extraction of template molecule, we used its platinum-bowl as bowl-shaped host in phosphate buffer solution.

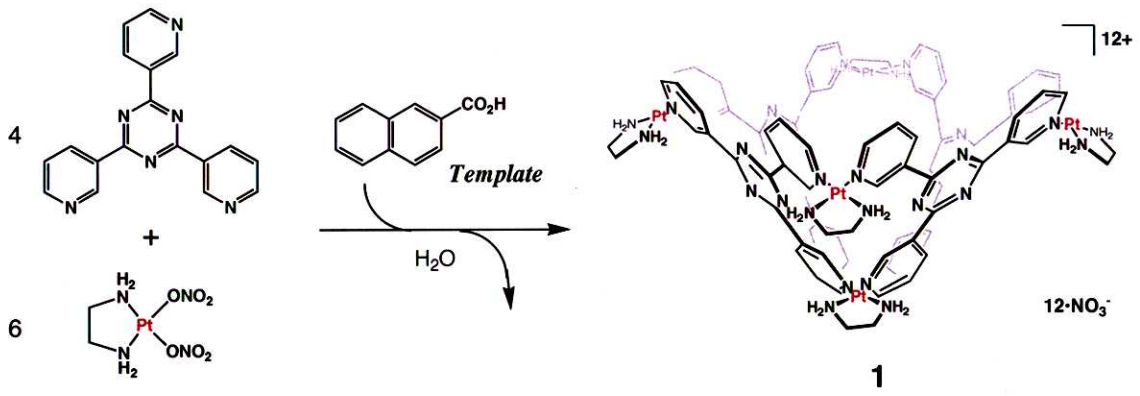

Scheme 1. Template-induced self-assembly of Pt-bowl shaped cavity **1**.

4.2.2 De novo design of nona-peptide **2**

Bowl-shaped host **1**[7] potentially capable of accommodating two or more amino acid residues. De novo designed oligopeptide **2** consists of only nine residues with two Trp at both terminals. Assuming α-helical conformation of **2**, hydrophobic indole rings of *i*, *i* + 8 Trp residues are oriented on the same face of the helix,[8] whereas negative charges of *i*, *i* + 4 Glu residues are on the opposite face (Scheme 2). Accordingly, the bowl complex **1** is expected to bind **2** in α-helical conformation through two types of host-guest interactions: primarily, hydrophobic interaction between the Trp residues and the pocket of **1** and, secondarily, electrostatic interaction between the Glu residues and the highly positive charge of **1** (12+). The remaining Ala residues have latent propensity for α-helical conformation. Despite of reasonable design of **2** for α-helical conformation, circular dichroism spectra showed that free peptide **2** took almost unordered structure due to shortness of peptide length.

4.2.3 ^{1}H NMR studies of complexation of **1** and **2**

In expectation of α-helix induction, **1** and **2** were mixed in an aqueous solution. When **1** (3 equiv) was added to 100 mM phosphate buffer solution of **2** (2.5 mM), we were disappointed to obtain a somewhat complex NMR spectrum from which the conformation of **2** could not be determined. However, upon the addition of a small amount of chloroform (1v/v%), the signals of **2** became simpler (Figure 1). All the nine residues of **2** were reasonably assigned by TOCSY and NOESY measurements. Most signals of **2** were upfield shifted, indicating the encapsulation of **2** within hydrophobic pocket of **1**. Indeed, some NOEs between **1** and **2** were observed. The Job's plot supported 1:1 complexation of **1** and **2** (Figure 2). From NMR titration, the association constant was estimated to be about 1 x 10^3 M^{-1} (Figure 3).

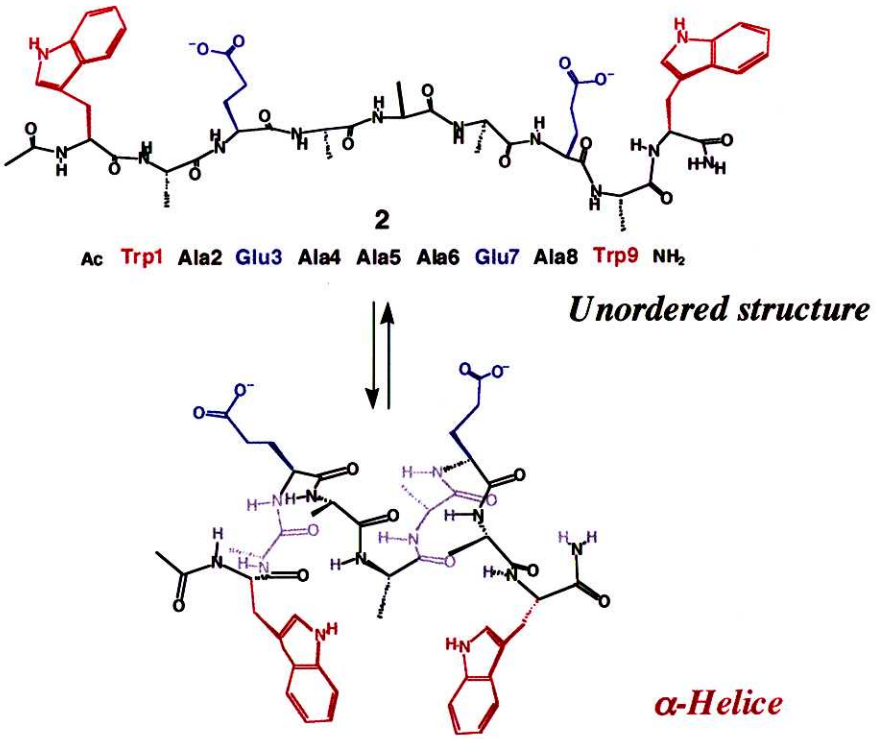

Scheme 2. De novo design of peptide **2** and equilibrium between unordered and α-helical structure

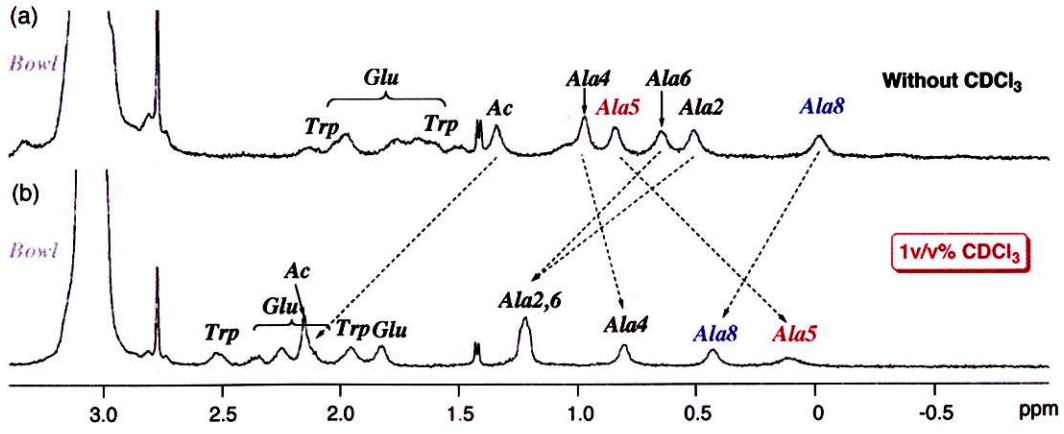

Figure 1. ^{1}H NMR spectra (500 MHz) of **1** and **2** in H_2O/D_2O (9/1; 100 mM phosphate buffer, pH 6.8). [**1**] = 7.5 mM, [**2**] = 2.5 mM. (a) Without $CDCl_3$. (b) With 1v/v% $CDCl_3$.

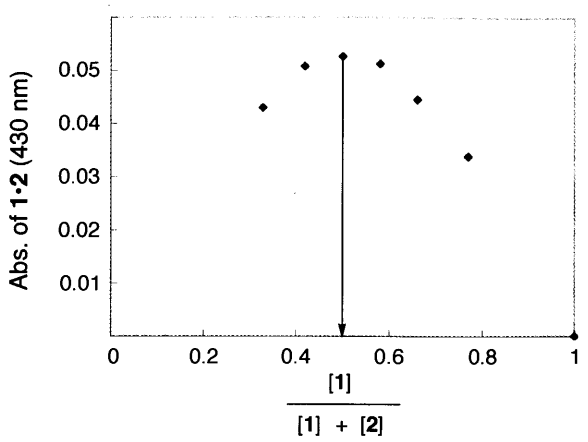

Figure 2. Job's plot of **1**·**2**. Concentration of **1**·**2** was estimated from CT absorption around 350-500 nm, that is specific to the complex **1**·**2** ([**1**]+[**2**] = 2.0 mM).

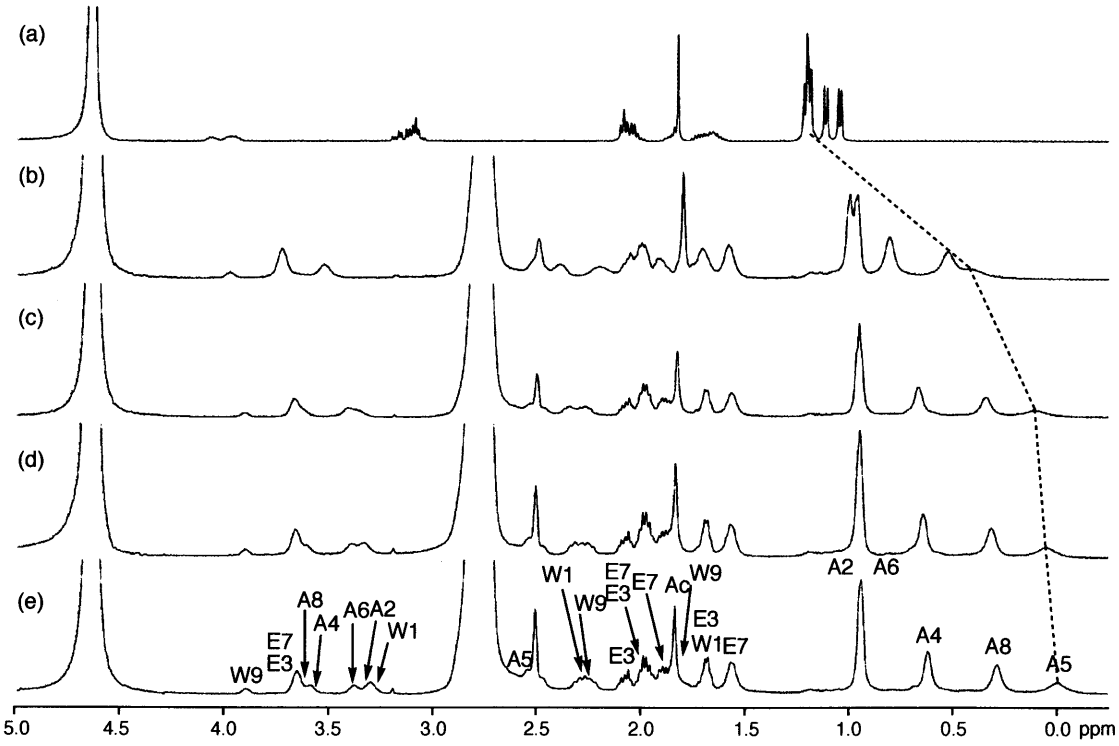

Figure 3. NMR titration of peptide **2** with **1** in the presence of 1v/v% chloroform. [**2**] = 2.5 mM and [**1**] = (a) 0 mM, (b) 2.5 mM, (c) 5.0 mM, (d) 6.3 mM and (e) 7.5 mM

The conformation of complexed **2** could not be discussed from CD measurement because strong absorption of **1** around 200-250 nm fatally interfered the CD of **2**. Thus, the α-helical conformation of **2** in the cavity of **1** was elucidated by careful NMR analysis. We noted that

the up-field shifts of the Hβ signals of Trp1, Trp9, and Ala5 residues (Δδ = ca. −1.2 ppm) were particularly larger than those of others, suggesting that these residues were co-enclathrated in the cavity of **1**. Namely, Trp1, Ala5, and Trp9 in *i*, *i*+4, and *i*+8 positions were oriented on the same face in good agreement with the α-helical conformation of peptide **2** (Figure 4).

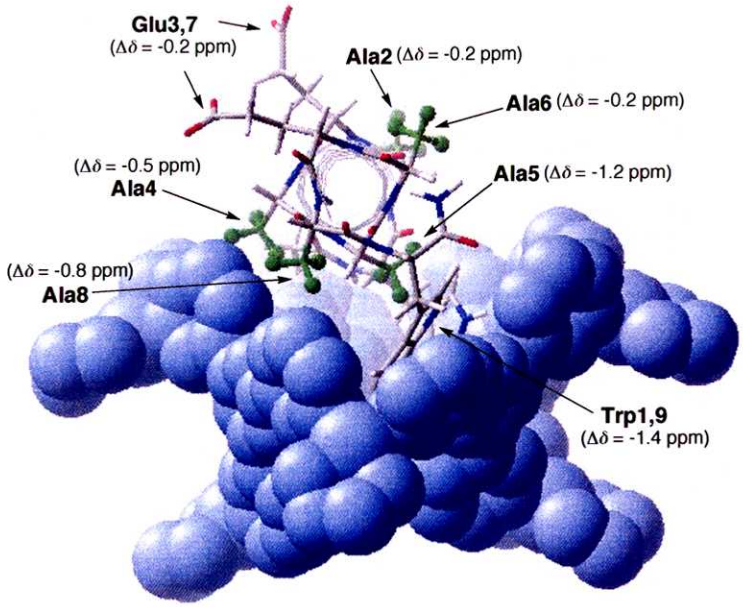

Figure 4. Comparison between α-helical conformation of bound **2** and chemical shifts. Values of Δδ are difference of Hβ chemical shifts from free peptide.

4.2.4 NOESY study of the conformation of bound peptide **2**

The α-helical conformation was more reliably confirmed by analyzing NOE cross-peaks of peptide **2**. Several medium range NOEs, for example, $d_{\alpha\beta}(i,i+3)$, $d_{\alpha N}(i,i+3)$ and $d_{\alpha N}(i,i+4)$ were observed in NOESY measurement, being characteristic to typical α-helical conformation (Figure 5). Some sequential $d_{NN}(i, i+1)$ NOESY cross-peaks also supported the helical structure.

The conformation of **2** was also studied by molecular dynamics (MD) simulation with CNS program[9] that run under NOE distance restraints (39 intra-residue + sequential, 25 medium-range). From the observed 68 NOE correlations, four unreasonable correlations presumably arising from very minor conformational isomers were eliminated for the CNS calculation. All of the 15 lowest-energy structures for **2** predicted the α-helical conformation (Figure 6). These ensembles showed low backbone pairwise RMSD (0.68 Å) and no violation of ideal bond length and angles. Since some NOEs were observed between Ala5 methyl and indole rings of both Trp residues, two indole rings were shown to be on the same face.

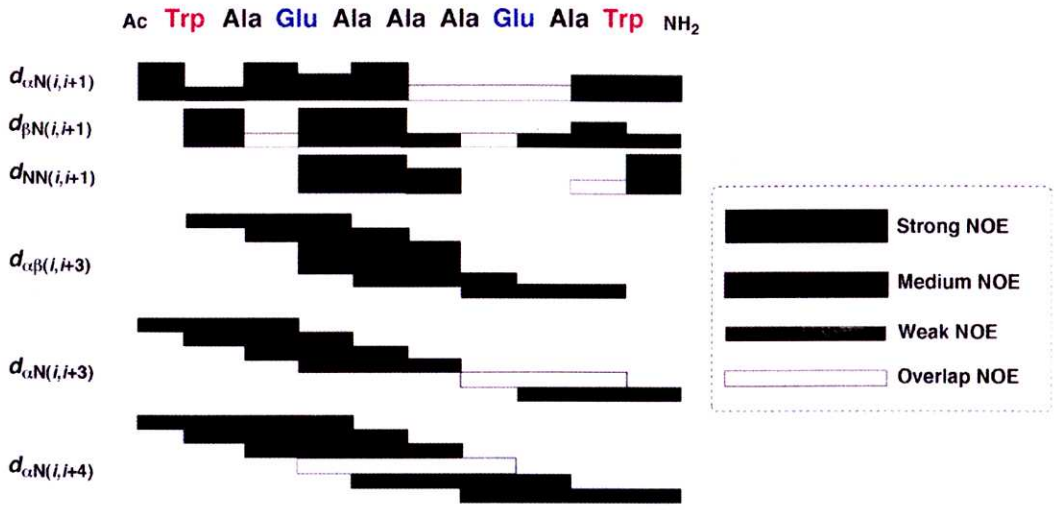

Figure 5. NOE correlations for bound peptide **2** in H_2O/D_2O = 9/1 (100 mM phosphate buffer, pH 6.8). Black bars indicate intensity of each NOE signals. White bars indicate ambiguous NOE signals due to fatal overlapping of cross-peaks.

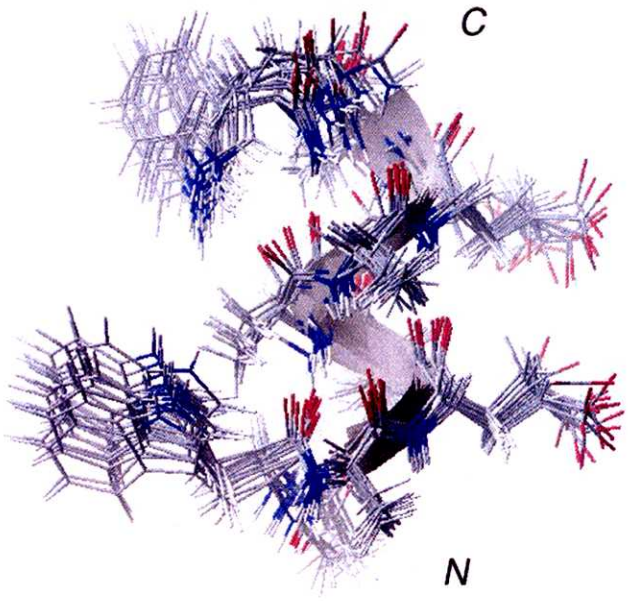

Figure 6. Superposition of 15 lowest energy structures by CNS[9] for bound peptide **2**.

4.2.5 Cα chemical shift comparison between bound and free peptide **2**

In NMR study of protein, secondary structures are also discussed from chemical shift of Cα.[10] Especially, this method is useful for small and flexible peptides, because chemical shift changes are averaged in a linear or direct manner in contrast to NOE, that is a very

nonlinear average of the conformational states involved. Although chemical shifts of ^{13}C were upfield shifted about 1ppm due to the shielding effect of bowl **1** (Cβ in Table 1 and 2), Cα shifts of most residues were over values used in determination of secondary structure in CSI (Figure 7).[11] This suggest that α-helical conformation of bound **2** was also supported from CSI.

Table 1. ^{13}C Chemical shifts[a] of bound peptide **2** (ppm).

Residue	Cα	Cβ
Trp1	59.6	28.4
Ala2	54.6	18.1
Glu3	57.9	29.1
Ala4	53.7	18.1
Ala5	?[b]	?[b]
Ala6	54.0	18.1
Glu7	57.9	29.3
Ala8	53.5	18.7
Trp9	55.7	28.4

[a]Determined from HSQC, relative to DSS as external standard.

[b]We couldn't assign those chemical shifts due to their low intensity.

Table 2. ^{13}C Chemical shifts[a] of free peptide **1** (ppm).

Residue	Cα	Cβ
Trp	56.4, 57.6	29.3
Ala	52.4	18.8
Glu	56.5	29.9

[a]Determined from HSQC, relative to DSS as external standard.

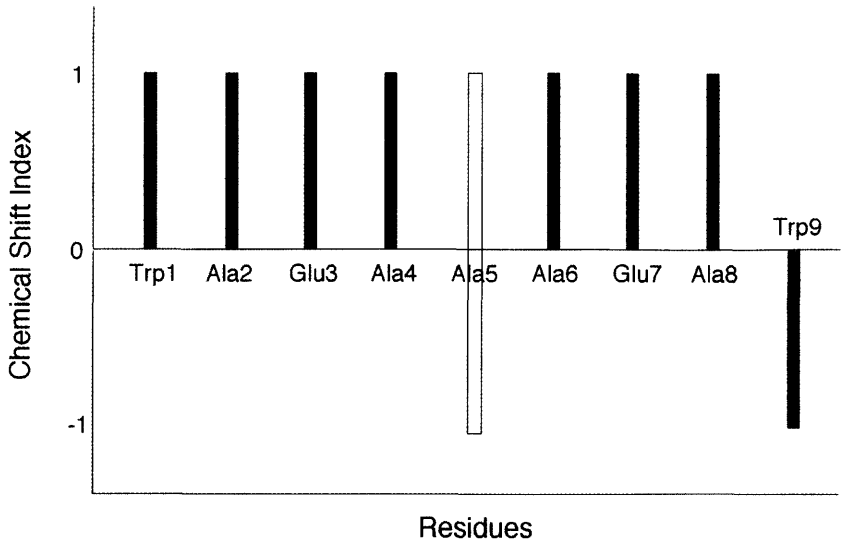

Figure 7. Chemical shift index plotted for the bound **2**. If the chemical shift is greater than the value used in determination of secondary structure, CSI is 1, and vice versa. Four consecutive 1's indicate that this regions have helical conformation.

4.2.6 Proposed structure of **1**·**2** complex

From the NMR studies, Job's plot, and the MD simulation, we conclude that oligopeptide **2** adopts α-helical conformation and Trp1, Ala5, and Trp9 on the same face of the helix are deeply accommodated in the cavity of **1** to form stable **1**·**2** complex as depicted in Figure 8. Chloroform, which is essential to the α-helix induction, is probably co-enclathrated in a small void surrounded by Trp1, Ala5, and Trp9 in **1**·**2** complex, though we could not specify the number and position of co-enclathrated chloroform molecules by NMR. Since chloroform shows very low solubility in water, titration experiment was difficult. Stabilization of α-helical conformation of **2** was observed when more than ca. 10 equiv chloroform was added to the solution.

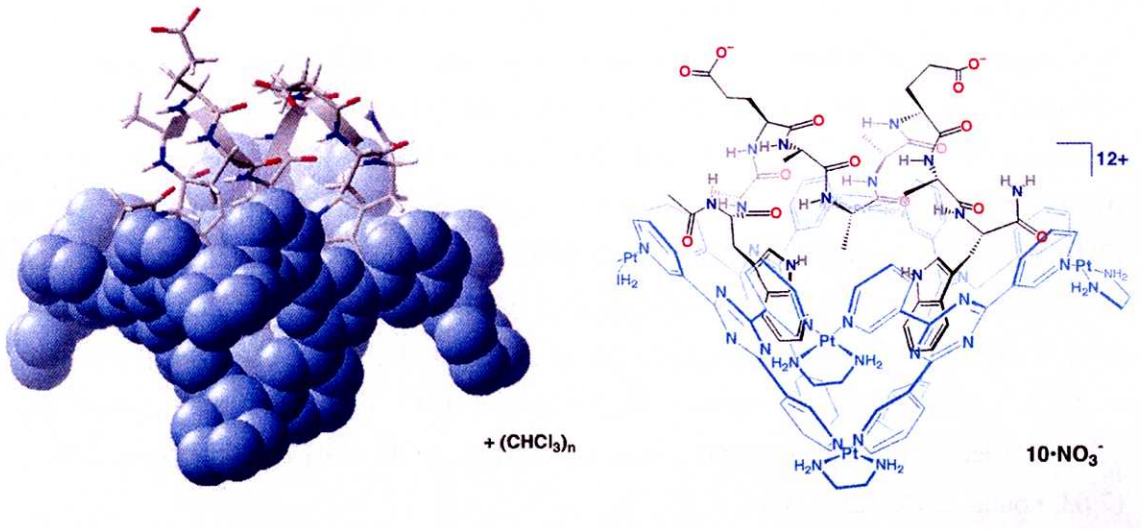

Figure 8. The proposed structure of complex **1**·**2**. (a) Bowl-shaped cavity of **1** and peptide **2** are represented by space-filling and cylindrical models, respectively. (b) Schematic representation of complex **1**·**2**.

4.3 Conclusion

In conclusion, we have demonstrated that bowl **1** has ability to induce and stabilize the α-helix conformation of a de novo designed peptide. It is worthy of note that the stabilization of secondary structures by hydrophobic environment is what nature is doing. Our bio-inspired method has potential applications for stabilizing not only other secondary structures but, ultimately, tertiary structures of proteins.

4.4 Experimental Section

Materials, peptide synthesis, procedure of UV titration, NMR measurements, Job's plot and structural calculation by CNS were described in General Experimental Section.

Synthesis and physical properties of platinum bowl-shaped cavity 1

2,4,6-tris(3-pyridyl)-1,3,5-triazine (0.20 mmol), (en)Pt$(NO_3)_2$ (0.30 mmol) and 2-naphthoic acid (0.25 mmol) as template were combined in H_2O (10 mL) and stirred for 6 days at 90 °C. After filtration, a small amount of nitric acid was added to the solution and its slightly acidic solution was washed five times with chloroform and over, then the solution was concentrated.

A large amount of acetone was added to the concentrated solution to give white precipitate. This precipitate was collected and washed with acetone. After drying, white powder was dissolved in water, then this solution was lyophilized (for complete evaporation of residual acetone). Yield 90%. ^{1}H NMR (500 MHz, D_2O, 300 K, TMS as external standard): δ 10.63 (s, 8H), δ 9.90 (s, 4H), δ 9.25 (d, J = 5.0 Hz, 8H), δ 9.19-9.14 (m, 16H), δ 7.87-7.81 (m, 12H), δ 3.02-2.86 (m, 24H). ^{13}C NMR (125 MHz, D_2O, 300 K, TMS as external standard): δ 169.2 (*C*q), δ 169.1 (*C*q), δ 155.6 (*C*H), δ 155.2 (*C*H), δ 153.5 (*C*H), δ 153.0 (*C*H), δ 140.6 (*C*H), δ 140.3 (*C*H), δ 134.3 (*C*q), δ 134.2 (*C*q), δ 127.7 (*C*H), δ 127.4 (*C*H), δ 47.7 (CH_2), δ 47.2 (CH_2). IR (KBr, cm^{-1}): 3066, 1608, 1587, 1533, 1384, 1320, 1192, 1175, 1053. Mp.: > 250 °C (dec). Elemental analysis calcd. for $C_{84}H_{96}N_{48}O_{36}Pt_6 \bullet 16H_2O$: C, 26.46; H, 3.38; N, 17.63. Found: C, 26.72; H, 3.44; N, 17.37.

4.5 References

1 For reviews of folding of secondary structures: (a) R. Parthasarathy, S. Chaturvedi, K. Go, *Prog. Biophys. molec. Biol.* **1995**, *64*, 1–54. (b) S. H. Gellman, *Curr. Opin. Chem. Biol.* **1998**, *2*, 717–725.(c) J. Venkatraman, S. C. Shankaramma, P. Balaram, *Chem. Rev.* **2001**, *101*, 3131–3152.

2 De novo design of helix: (a) K. R. Shoemaker, P. S. Kim, E. J. York, J. M. Stewart, R. L. Baldwin, *Nature*, **1987**, *326*, 563–567. (b) S. Marqusee, R. L. Baldwin, *Proc. Natl. Acad. Sci. USA* **1987**, *84*, 8898–8902. (c) P. C. Lyu, M. I. Liff, L. A. Marky, N. R. Kallenbach, *Science* **1990**, *250*, 669–673. (d) S. Padmanabhan, S. Marqusee, T. Ridgeway, T. M. Laue, R. L. Baldwin, *Nature* **1990**, *344*, 268–270. (e) D. H. Appella, L. A. Christianson, D. A. Klein, D. R. Powell, X. Huang, J. J. Barchi Jr, S. H. Gellman, *Nature*, **1997**, *387*, 381–384.

3 De novo design of β-sheet structures: (a) M. R. Ghadiri, J. R. Granja, R. A. Milligan, D. E. McRee, N. Khazanovich, *Nature*, **1993**, *366*, 324–327. (b) F. J. Blanco, M. A. Jiménez, J. Herranz, M. Rico, J. Santoro, J. L. Nieto, *J. Am. Chem. Soc.* **1993**, *115*, 5887–5888. (c) T. S. Haque, S. H. Gellman, *J. Am. Chem. Soc.* **1997**, *119*, 2303–2304. (d) N. Sakai, N. Majumber, S. Matile, *J. Am. Chem. Soc.* **1999**, *121*, 4294–4295. (e) N. Sakai, S. Matile, *Chem. Commun.* **2003**, 2514–2523.

4 Covalent link: (a) D. Y. Jackson, D. S. King, J. Chmielewski, S. Singh, P. G. Schultz, *J. Am. Chem. Soc.* **1991**, *113*, 9391–9392. (b) C. Bracken, J. Gulyás, J. W. Taylor, J. Baum, *J. Am. Chem. Soc.* **1994**, *116*, 6431–6432. (c) E. Cabezas, A. C. Satterthwait, *J. Am.*

Chem. Soc. **1999**, *121*, 3862–3875. (d) C. E. Schafmeister, J. Po, G. L. Verdine, *J. Am. Chem. Soc.* **2000**, *122*, 5891–5892. (e) R. N. Chapman, G. Dimartino, P. S. Arora, *J. Am. Chem. Soc.* **2004**, *126*, 12252–12253.

5 Metal-coordination: (a) M. R. Ghadiri, C. Choi, *J. Am. Chem. Soc.* **1990**, *112*, 1630–1632. (b) F. Ruan, Y. Chen, P. B. Hopkins, *J. Am. Chem. Soc.* **1990**, *112*, 9403–9404.(c) M. J. Kelso, H. N. Hoang, W. Oliver, N. Sakolenko, D. R. March, T. G. Appleton, D. P. Fairlie, *Angew. Chem.* **2003**, *115*, 437–440. *Angew. Chem. Int. Ed.* **2003**, *42*, 421–424. (d) A. Ojida, M. Inoue, Y. Mito-oka, I. Hamachi, *J. Am. Chem. Soc.* **2003**, *125*, 10184–10185.

6 Other interactions: (a) M. W. Peczuh, A. D. Hamilton, J. Sánchez-Quesada, J. de Mendoza, T. Haack, E. Giralt, *J. Am. Chem. Soc.*, **1997**, *119*, 9327–9328. (b) Y. Inai, K. Tagawa, A. Takasu, T. Hirabayashi, T. Oshikawa, M. Yamashita, *J. Am. Chem. Soc.* **2000**, *122*, 11731–11732. (c) D. Wilson, L. Perlson, R. Breslow, *Bioorg. Med. Chem.* **2003**, *11*, 2649–2653. (d) A. Verma, H. Nakade, J. M. Simard, V. M. Rotello, *J. Am. Chem. Soc.* **2004**, *126*, 10806–10807.

7 Pd-bowl complex: (a) M. Fujita, S.-Y. Yu, T. Kusukawa, H. Funaki, K. Ogura, K. Yamaguchi, *Angew. Chem.* **1998**, *110*, 2192–2196. *Angew. Chem. Int. Ed.* **1998**, *37*, 2082–2085. (b) S.-Y. Yu, T. Kusukawa, K. Biradha, M. Fujita, *J. Am. Chem. Soc.* **2000**, *122*, 2665–2666. (c) M. Yoshizawa, T. Kusukawa, M. Fujita, S. Sakamoto, K. Yamaguchi, *J. Am. Chem. Soc.* **2001**, *123*, 10454–10459.

8 Ideally, Trp resides should be located at *i*, *i* + 7 positions. We originally designed peptide **2** so that it is encapsulated within dimeric capsule of **1**, which we have previously reported.[7b] In this study, we unexpectedly observed the binding of **2** by monomeric **1**. Despite of the subtle mismatch in the location of Trp positions, α-helical conformation of **2** was sufficiently stabilized because of flexible orientation of terminal Trp residues.

9 A. T. Brünger, P. D. Adams, G. M. Clore, W. L. DeLano, P. Gros, R. W. Grosse-kunstleve, J.-S. Jiang, J. Kuszewski, M. Nilges, N. S. Pannu, R. J. Read, L. M. Rice, T. Simonson, G. L. Warren, *Acta Cryst.* **1998**, *D54*, 905–921.

10 D. S. Wishart, B. D. Sykes, F. M. Richards, *Biochemistry* **1992**, *31*, 1647–1651.

11 D. S. Wishart, B. D. Sykes, *Methods Enzymol.* **1994**, *239*, 363–392.